CRITICAL REVIEW

A state of the art on surface morphology of selective laser-melted metallic alloys

Mustafa Kuntoğlu[1] · Emin Salur[2] · Eyüb Canli[1] · Abdullah Aslan[1] · Munish Kumar Gupta[3,4] · Saad Waqar[5] · Grzegorz M. Krolczyk[3] · Jinyang Xu[6]

Abstract

The possibility of producing complex metallic parts in various industries can be attributed to the selective laser melting (SLM) additive manufacturing method. As a powder bed fusion technique, SLM fabricates the product layer by layer. The state-of-the-art research on SLM, the metallic alloys utilized in the process, and the surface morphology of fabricated parts are discussed in this paper. The present report contributes to the literature by providing a comprehensive overview of the surface morphology of metallic alloys fabricated using the SLM additive manufacturing method. The article covers recent research on SLM, metallic alloys used in the process, and the surface morphology of fabricated parts. Insights into the challenges and opportunities of SLM for the fabrication of metallic parts with desired surface properties are provided. In the first part, parameters representing surface morphology are introduced and types of surface defects are viewed. Subsequently, influence of process variables during the production phase is discussed in-depth, overviewing several parameters such as laser, scanning, and geometric parameters. Surface morphology enhancement, namely in situ treatment, post-processing, and finishing-machining techniques, is viewed separately by classifying them into subtopics, in respect of their improvement effectiveness. Mechanical aspects of the microstructure and surface are evaluated in correlation with the surface morphology. The discussion of the findings considering the advantages and disadvantages of this technology is summarized finally. It is concluded that laser parameter effect's significance depends on the work alloy. In the literature, process parameters are systematically studied, and better surface quality and favourable surface morphology of as build surfaces are possible. Moreover, it has been concluded that the surface morphology and quality of SLMed products can be improved with in situ techniques and post-treatments. Relieving residual stresses and decreasing porosity on the surface (various types of holes, pinholes, vacancies, etc.) during SLM operation are possible by base plate heating, powder preheating, and re-scanning. It is also noticed that the machinability studies of SLMed parts mainly focus on mechanical machining such as grinding and milling. Studies on the correlation between surface morphology of SLMed parts and mechanical properties are relatively scarce comparing to works on SLM production parameters. Finally, as an emerging technology for vast production of industrial items, it is concluded that surface morphology of SLMed products needs systematic correlation studies between process parameters and surface results.

Keywords Additive manufacturing · Metallic alloys · In situ treatment · Post-treatment · Selective laser melting · Surface morphology

1 Introduction

Selective laser melting (SLM) is a powder bed fusion (PBF)–based additive manufacturing technique [1]. In SLM, a high-power laser beam is used in order to selectively melt powder particles [2]. These molten powder particles join together and resolidify to form the desired shape

Extended author information available on the last page of the article

along the laser trajectory. Same process is repeated layer by layer until the final geometry is attained [3]. This method is preferred to produce high-density metallic, ceramic, or composite material components with enhanced mechanical properties [4]. Moreover, general advantages of additive manufacturing techniques make this method attractive since it accelerates production. SLM proven its worth when geometrically complex components need to be produced in a short time [5]. A schematic representation of SLM is

shown in Fig. 1. It is an innovative approach having higher efficiency and maximum flexibility to offer near-net shape products according to requirements. Since metallic alloys cover a wide range of engineering applications, components produced with this method can serve to a broad field [6]. On the other hand, SLM is highly and recently studied for numerous conventional and innovative aspects that may lead to dramatical advantages that make the method more prominent. For instance, the method can be a remedy for recycled metal utilization [7]. The cited work uses XPS (X-ray photoelectron spectroscopy), XRD (X-ray diffraction), and SEM (scanning electron microscopy) techniques to characterize virgin and recycled metallic powders for 3D printing applications. The authors aim to understand the chemical and structural changes that occur during the recycling process and their impact on the properties of the powders for use in 3D printing.

The quality of a product is reflected by several indicators including surface roughness, morphology, and mechanical features [8–10]. Considering sustainability, precision, geometrical constraints, and longer component lifetime, surface morphology becomes one of the most important outputs in production chain [11, 12]. Although it is possible to fabricate high-density, flexible, and near-net shape parts with SLM, there is a challenge about product surfaces. Unlike the traditional manufacturing methods, SLM enables the fusion of particles to compose layers one by one [13]. This procedure creates surfaces resembling to ones from welding process due to interaction between layers of particles [14]. The characteristics of the fusion work depend on the process variables, namely laser power, scanning speed, scanning pattern, and geometry. In this paper, a review of the process variables affecting the surface morphology is outlined as well as the post-processing and mechanical aspects in respect of the surface morphology. Although there are different types of reviews about SLM in literature, none of them focused on the surface morphology of metallic alloy components processed through SLM in particular. This makes the review

first in the field. It is anticipated that the paper will serve as an essential guide for the researchers in the future. Types of surface defects and surface morphology representative parameters are summarized in the first section. Afterwards, process parameter–induced variations in surface morphology, surface morphology enhancement of SLMed metallic alloys, and surface morphology–induced variations in the behaviour of SLM components are extensively explained, respectively, before the concluded remarks, challenges, and future work sections. Investigated topics and subtopics of the scope designed for this study are outlined in Fig. 2. Each item in the diagram is discussed in the present paper with citations to the recent resources under respected sections.

1.1 Types of surface defects

Although additive manufacturing methods operate the process without requiring machining tools, procedures, and apparatus, they have a number of challenges and in situ problems during production [15, 16]. As a result of process parameters, various surface defects occur, which may influence the application and mechanical properties of the component during its lifetime. The processing parameters included in SLM are mainly laser power, scanning speed, hatch spacing, layer thickness, and scanning pattern. All of these parameters, either collectively or separately, have significant influences on the surface quality and defect formations such as porosity, fusion hole, balling, microstructural defects, morphological irregularities due to residual stresses, micro-cracks, spalling, leaves, dimples, and spatter [17]. The types of surface defects are demonstrated in Table 1 in order to identify them visually and to provide the reader clarity about terminology that is used in the rest of the paper. For instance, the porosity formations exist as small size and spherical shape blanks that are usually generated as a result of accumulated gas during the preparation of powders and they stay on the molten pool before solidification without solving due to high cooling rates [18]. Fusion holes

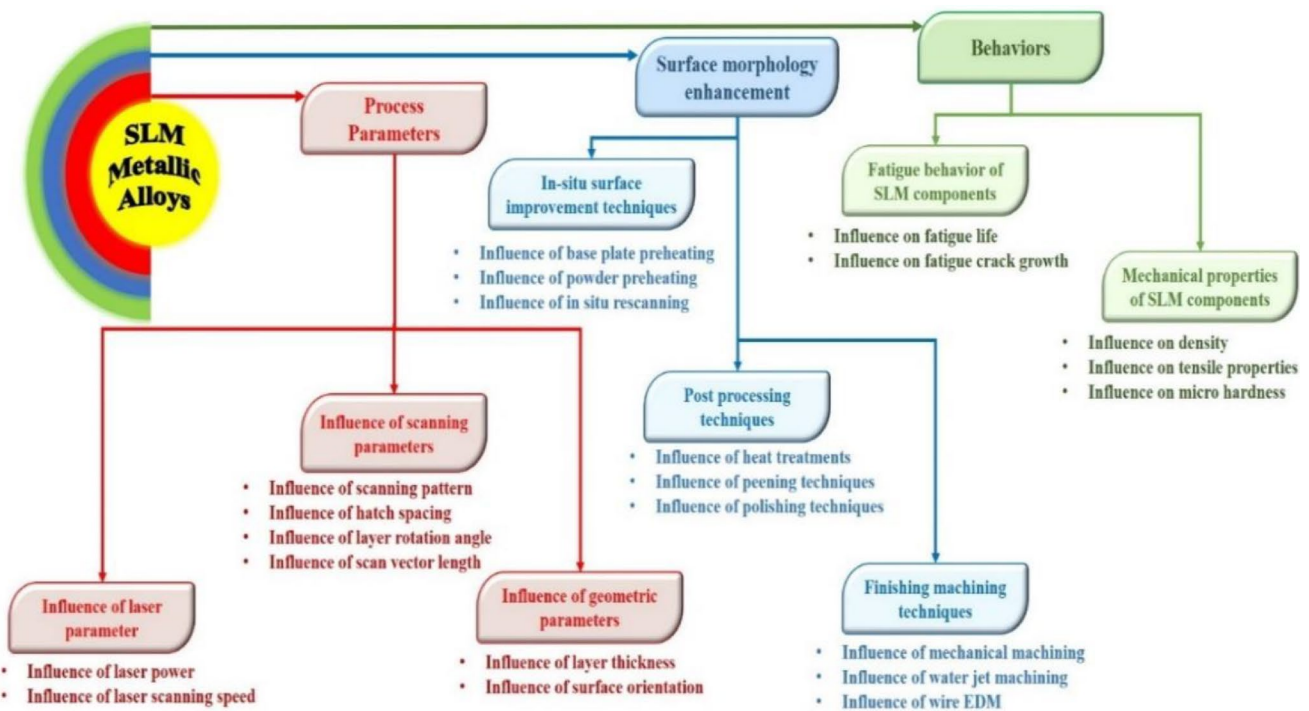**Fig. 1** Schematic representation of a SLM operation and produced part
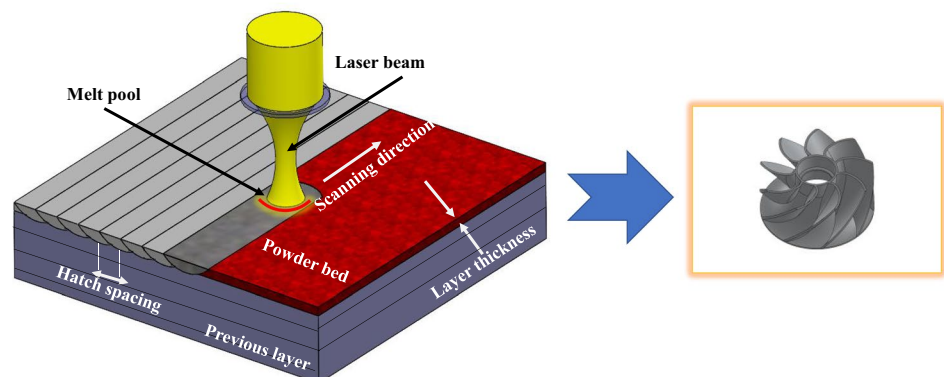
Fig. 2 Investigated topics and subtopics of the scope designed for this study

form as a result of incomplete process due to the insufficient melting of powders [19]. Cracks are formed as a result of local energy build-up and due to high cooling rates and high temperatures during the process leading to thermal stresses [20]. Spatter is a residue on the final layer, which is realized due to interaction between laser and powder material during fusion, as some particles scatter to various directions outside of the laser track [21]. Rapid cooling of laser tracks, in the existence of conjugate heat transfer and thermal radiation, interacts with previous tracks having residual stresses and can create spalling, leaves, and micro-cracks [22]. Most of the surface irregularities such as incomplete spreading, satellites, patters, and dimples on the final layer are residues powder fusion by the laser.

1.2 Surface morphology representative parameters and measurement techniques

Surface morphology is an important feature of products, from micro- to macro-scale, for several application aspects such as suitability of wettability, adhesion properties, tribological properties, lamination, corrosion resistance, and topological integrity. As a promising production method, SLM should be discussed in terms of surface morphology metrics. SLM produces near-net shape complex components through the fusion of molten powder particles. However, it can also cause certain surface defects that can significantly reduce surface quality [26]. The prominent surface

defect and surface morphology aspects, also summarized in Table 1, were researched based on the existing literature and a systematic behaviour and relationship with various process parameters are discussed in Sect. 2. Existing state of the art on surface modification techniques including in situ techniques and post-processing methods is summarized in Sect. 3, whereas the surface morphology and defects induced variations in mechanical behaviours of SLM fabricated components are considered and explained in Sect. 4. The literature review shows that porosity, density, hardness, surface roughness, and surface profile cumulatively result in surface morphology of a SLM product [24–26, 36–44]. In order to provide desired surface properties for SLM products, predetermined operational parameters should be ensured for consistent structure at micro- and macro-scale. Since the material is composed point by point, line by line, and layer by layer, it is reasonable to expect surface defects as a result of building phases during the fabrication process, due to SLM parameters. Relative density of a SLM product sample is one of the indicative measures. The residual gas among particles during the manufacturing process influences the packing performance and leads to vacancies during solidification phase. Pore is one of the examples of vacancies as being an undesired structural formation on the surface which can be detected with microscopic images. The distribution and packing mechanism of powder throughout the layers greatly impact the hardness and surface roughness of the material. Surface profilometers and hardness

Table 1 Type of surface defects

Ref	Types of Surface Defects	Figure		
[23] [24]	Porosity			
[25] [26]	Fusion Hole			
[23] [27] [24]	Balling			
[28] [29]	Microstructural Defects			
[30] [31] [32]	Cracking			

measurement devices can be used in order to evaluate the surface roughness and hardness after the SLM process. Atomic force microscope can also be utilized for determining surface profiles. On the other hand, the surface profile measurement depends on the topography of the measured area providing the high-density data of the 3D model of the surface [44]. The surface texture is determined by several parameters such as arithmetic mean height and maximum valley height. The measurement of this 3D surface was done by means of confocal microscopy [45] and coherence scanning interferometry [46]. As a summary of the surface morphology representative parameters and their respected

Table 1 (continued)

measurement methods, Fig. 3 is given. Items in Fig. 3 have literature examples that are cited in the above and following text of the paper.

In general, surface morphology indicators are surface profiles, roughness values, porosity values, and patterns. The examination of surface morphology is done by imaging at different scales from scanning electron microscope (SEM) to micro-meter scale microscopes, profilometers, and scanners. The structure of the present review paper uses morphology indicators that are obtained from surface examination tools for evaluating investigation parameters that are reported in the literature papers. Initially, the influence of SLM process parameters was discussed followed by various techniques to enhance and control the surface morphology. In the end, relationship between surface and various characteristic mechanical behaviours was established.

Fig. 3 Surface morphology representative parameters and measurements
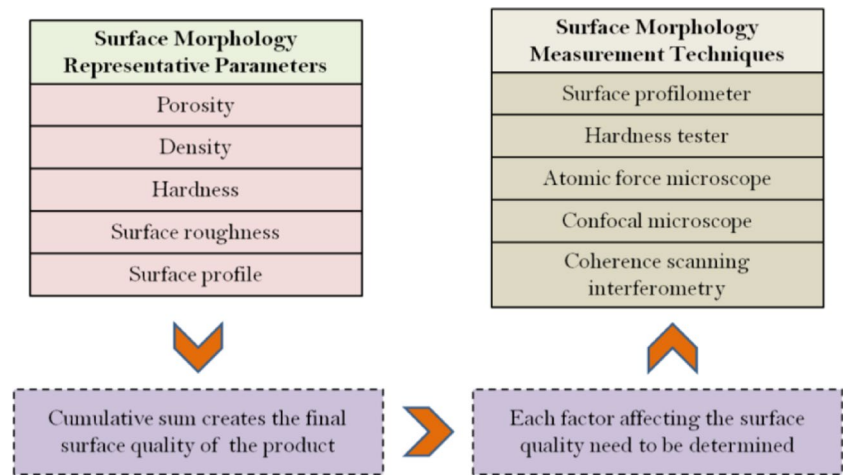
2 Process parameter–induced variations in surface morphology

Despite its many advantages, manufacturing with SLM has various challenges that directly affect the quality of the product and surface in particular. In order to overcome the reduced surface quality and other material defects such as pores, voids, and cracks, processing parameters have been extensively investigated in the past. The effects of laser power, scanning speed, scanning strategies, and geometric parameters are the prominent factors affecting the surface morphology of as-build SLM products. The SLM operational parameters affecting surface morphology are listed in Table 2 with literature instances and their general effects.

2.1 Influence of laser parameters

Being one of the promising additive manufacturing methods, SLM has paved the way for increased automation in manufacturing industries for producing complex parts [86–88]. Complexity can be solved by the application of SLM with high density and accuracy using the point-by-point production method; however, this somehow brings faults in material structure, and eventually on the surface. For desired surface morphology, continuous melting and densification need to be obtained during creating layers of a part. The laser beam used for melting of powders is set to a level of power and speed, which influences the densification behaviour and the area and depth of the melt pool. As a microstructural characteristic, surface morphology is essentially determined by laser power and laser scanning speed at the beginning of the building of the product. In addition, the contact angle, contact zone, and track width of the laser beam need to be optimized. Accurate selection of laser parameters enables fabricating fully dense parts from core to edge on s specific track. Otherwise, unstable contact conditions lead to undesired geometry, surface defects, spatters, and reduced surface

quality. Nevertheless, it is noteworthy that parts fabricated by SLM sometimes needs additional surface finishing operations [26].

2.1.1 Influence of laser power

Laser power directly affects the input energy and hence responsible for the melting and densification phenomena. According to Zhao et al. [56], laser power has a great impact on the determination of the size of the melt pool in terms of width and depth. Melt pool dimensions, in turn, controls the material microstructure, porosity, and density. Also, material discontinuity shows itself with surface defects and is created by incomplete melting or early densification. In [54], the authors highlighted that poor forming performance is obtained with lower power input. Recently, considerable numbers of investigations have been focused on the influence of laser power. Liu et al. [48] presented a study based on the investigation of laser energy input for determining the effects of laser power on surface roughness and hardness by response surface methodology. According to the analysis of variance results, laser power has a high and fluctuating effect on surface roughness. On the other hand, laser power influence hardness negatively. According to Sing et al. [49], the melt pool area is highly influenced by laser power in the horizontal dimensions. High laser power comprises a stable melt pool which results in improved surface quality. Also, high laser power increases microhardness, which is related to lower porosity and its intensifier effect of strength. Lin et al. [27] indicated that when laser power is low, insufficient fusion of powders lead to irregular surface texture with increasing surface roughness. It was stated from the previous studies [53] that increasing laser power directly related to the increased energy transfer in to the powder bed, facilitating fusion mechanism and densification. However, it is also stated that excessive power may cause cracks and delamination. In [89], it is stated that a larger melt pool and

Table 2 SLM process parameters affecting surface morphology

Ref	SLM Parameters	Work Material	Related Surface Measures	Effect Assessment
[47]	Laser Power+Scan Speed	316 L Stainless Steel	Surface defects	Laser power and scan speed parameters both have optima. Higher and lower values of the optima give undesired values of the investigated surface measures. Each alloy changes the optima
[48]		316 L Stainless Steel	Surface Roughness, Hardness	
[49]		Titanium, Tantalum	Relative Density, Microhardness	
[28]		Ti6Al4V	Densification, Surface Defects	
[50]		AlSiMg10	Surface Roughness, Surface Defects	
[24]		Al-Si Alloy	Densification, Surface Defects	
[31]		Ti-47Al-2Cr-2Nb	Density, Surface Defects	
[51]		Ti-Al6-4 V	Surface Roughness	
[52]		Inconel 625	Surface Roughness	
[53]	Laser Power	AlSiMg10	Densification Behaviour	Laser power seems to be the most investigated SLM parameter
[54]		Co-29Cr-6Mo	Surface Defects, Thermal Condition	
[55]		A357 Al Alloy	Density, Structural Analysis	
[56]		Ti6Al4V	Solidification Behaviour	
[30]		316 L Stainless Steel	Surface defects, Density, Fatigue, Microhardness	The abundant industrial material library also necessitates investigation of laser power for proper fusion work
[36]		316 L Stainless Steel	Hardness, Surface Roughness, Surface Defects, Porosity	
[27]		AlSiMg10	Relative Density, Surface Roughness	
[57]		Ti	Densification, Surface Defects, Hardness	
[23]	Hatch Spacing	316 L Stainless Steel	Microstructure, Densification, Surface Defects	Laser tracks are in different phases as scanning pattern and scanning speed changes. Therefore, the distance between hatches effectively changes conjugate heat transfer and residues on the previous tracks. The heat transfer and cooling of the active track also interact with the residual stresses of the previous tracks
[58]		316 L SS	Temperature Distribution, Melt Pool Size, Microstructure, Overlap Rate, Surface Roughness, Relative Density	
[57, 59]		Ti-Al6-4 V	Temperature Distribution, Volume Shrinkage	
[24, 60]		17-4PH	Microhardness, Mechanical Properties	
[61]		Ti-Al6-4 V	Microstructure	
[62]		Ti6Al4V	Residual Stress	

Table 2 (continued)

Ref	SLM Parameters	Work Material	Related Surface Measures	Effect Assessment
[63]	Scanning Pattern	Inconel 718	Solidification	Conventionally, scanning is done by a single direction with parallel tracks at constant hatch spacing. However, literature shows that surface related problems can be eliminated by imposing innovative scanning patterns since previous works identified problems associated with conventional scanning
[64]		Ti64	Residual Stress	
[65]		Ti6Al4V	Molten Pool Dimension, Residual Stress	
[66]		AISI H13	Residual Stress	
[67]		Al Alloy EN AW 2618	Fractographic Analysis, Metallographic Analysis, Mechanical Properties	
[68],		-	Residual Stress	
[69]		316L Stainless Steel	Densification, Microstructural Defects	
[70]		304L stainless steel	Residual Stress	
[71]		-	Residual Stress	
[72]		X3NiCoMoTi 18–9–5	Residual Stress	
[73]		Ti6Al4V	Residual Stress	
[32]		Nickel Superalloy	Crack Analysis, Pore Analysis, Microstructure, Density	
[4, 61]		AlSi10Mg	Surface Roughness	
[74]	Layer Rotation Angle	Al-Si-10 Mg	Density	Residual stresses impose surface profile patterns of SLM products. Layer rotation angle have effects on the accumulation of those profiles
[75]		Al-Si-10 Mg	Microstructure, Densification, Microhardness, Residual Stress, Surface Profile	
[76]		In738LC	Texture and microstructural analysis	
[40]		EOS 17–4 PH stainless steel powder	Surface Profile, Surface Roughness	
[41]		Ti–Al6-4 V	Surface Profile, Surface Roughness	
[77]	Scanning Vector Length	austenitic steel 316L	Surface Roughness	
[50]		AlSi10Mg	Surface Roughness	Surface profile negatively affected after designated vector length values due to increased residual stresses
[78]		Al-Si-10 Mg	Residual Stress	
[79]		Ti6Al4V	Residual Stress	
[80]	Layer Thickness	904L Stainless Steel	Surface Defects	Thicker melt pool leads to balling, fusion holes, and porous surfaces
[81]		Magnesium	Surface Defects	
[82]	Surface Orientation	Ti6Al4V	Surface Roughness	Surface orientations other than horizontal and vertical arrangements, and complex surfaces are challenges for regular scanning
[83]		Ti	Surface Profile	
[84]		Inconel 625	Surface Roughness	
[85]		Ti6Al4V	Surface Defects, Microstructure, Surface Profile	

smaller shaped pores can be obtained with increasing power and energy input. Besides, pores increase with high power resulting in lower density in the material structure. According to Dursun et al. [47], low laser power may result in a lack of energy density, and with higher laser power, smooth tracks can be created, reducing surface roughness. Sun et al. [28] researched the effect of laser power and indicated that increased laser power accelerates the degree of melting and enhances the error rate in the building direction of the part. Cherry et al. [36] worked on surface roughness, hardness and porosity in order to research the effect of laser power. According to the authors, optimum results can be achieved laser power optimum level. Yang et al. [50] found that high power produces a more smooth surface. Kang et al. [24] demonstrated that high laser power enhances relative density, and over a range of laser power values, porous structure and balling effect are observed. Liverani et al. [30] stated that increasing power level increases material density, which is an indicator of reduced defect and porosity, and increased surface morphology. It can be concluded that according to the other influencer parameters, applied power range can either affect surface morphology favourably or adversely. It is needed to determine optimal laser power value specifically to the operation and material, for obtaining improved relative density, surface roughness, hardness, and minimum defects. Laser power determines the amount of focused energy into an area and affects further events such as melting, bonding and solidification. Viewed literature papers generally suggest higher laser powers for better surface morphology and quality. However, feasibility and cost aspects of such propositions are seldom addressed. Since laser power cannot be regarded as the only parameter and its effects in combination with other SLM parameters are still not very clear, there is still need for parametric investigations for generalization.

2.1.2 Influence of laser scanning speed

Starting from initialization of a SLM operation, the laser scans an area that is melted with laser power, and the laser speed determines the time for which the laser stays at a point [90]. Basically, solidification process at a targeted area with molten pool has not ended yet affects neighbouring powders and previous tracks depending on the scanning speed. Unlike the laser power, which determines the energy transferred to the target area, scan speed determines the energy transfer to the proximity of the target area. The shape of the molten pool transforms from spherical to slender with lower scanning speeds. [50]. Intrinsically, SLM mechanisms cannot maintain scan speeds when changing track direction. When scan speed becomes relatively lower during direction changes, low scan speed leads to surface tracks with more roughness. There are several works in the literature dedicated to SLM laser scan speed. In [48], a critical scan speed

is given. Below that value, surface quality drops significantly. In addition, scanning speed is found as the primary factor and reported to affect the hardness positively. Sing et al. [49] indicated laser speed as one of the influential factor for horizontal scanning. The authors state that decreasing scanning speed creates scan tracks and increases surface roughness. They also detected that lower scan speed results in increased microhardness leading to higher strength. Dursun et al. [47] demonstrated that large holes and voids are seen on the surface with increasing scanning speed. Sun et al. [28] reported that applying lower scanning speeds creates a completely dense structure under the surface but at higher speeds; unmelted powder leads to disordered texture and comprises balling effect. On the other hand, lower scanning speed produces a high dimensional error, reducing the part quality in a significant manner. It is referred from [24] that relative density is not changed with increasing scanning speed. The authors also suggest that porosity increases, and surface morphology deteriorates due to the partially melted particles. In [31], it is found that high scanning speed with low power produces balling and cracking, distortions and irregularities. Scanning speed identifies the focusing time of the laser beam to a particular zone, and it influences the melted pool size, joining mechanism, and surface characteristics together with the laser power. Excessive or deficient penetration resulting from inappropriate speed is seen to result in defects and insufficient fusion in the material according to the literature. Laser scan speed and laser power are the two fundamental SLM parameters for surface morphology of the products. They are projected to be investigated in the future considering different alloys and different application fields.

2.2 Influence of scanning parameters

The parts produced with SLM require a strategic plan to reach the final shape with good mechanical properties and surface characteristics [91]. The main consideration is to obtain high relative density determined by scanning parameters such as pattern, hatch spacing, layer rotation angle, and scan vector length. These factors influence bonding types of the powders and related material structures, which directly affect material and surface quality. The chemical reaction between powder particles is triggered and accelerated with applied laser power which transforms radiation to heat energy and increase temperature of the powders leading to bonding. Therefore, there is a need to identify the starting point, edge of the melt pool, surface of the part and scan direction for building operation. In addition to the production process, the interactions between in situ parameters have great importance on the arrangement of powders; melt pool, temperature development, and solidification time in the field. Correct scanning parameter selections enable acceptable

residual stress profiles [92]. Since the temperature gradient mechanism and cool-down phase act in the first place on residual stress formation, they can be optimized altogether [93]. Scanning parameters are evaluated in three subtitles.

2.2.1 Influence of scanning pattern

Among others, scanning pattern is the most investigated scanning parameter by the researchers in the field. Considering numerously reported scanning pattern strategies, Fig. 4 summarizes prominently published examples. Each scanning strategy is tried to be mentioned with its respected citation by the recent literature works in this section. The scanning pattern significantly influences residual stresses because of the applied laser beam alignment from beginning to end. Residual stresses impact the ultimate strength, structural integrity, isotropic material density, and performance during the utilization of a product. Also, increasing residual stresses enhance the pores and voids on the surface. Moreover, it also leads to premature cracking, delamination, and other structural defects even during the fabrication process. Eventually, scanning pattern determines the surface profiles at the final layer. One of the important side effects of scanning patterns is the overlap region which may change the structure of generated lines and surfaces. For comparing the overlap region, Almangour et al. [69] found that cross-hatched strategies provide the highest densification. In literature, zigzag, spiral in, spiral out [68]; perimeter first, edge to edge [70]; the island [32]; meander [67]; successive chessboard, most minor heat influence, and successive [66]; line [65]; horizontal [64], unidirectional and alternate [62]; and bidirectional [63] scanning strategies have been identified and applied to different types of powders for improved surface characteristics. The findings from previous literature can be explained as a successive strategy provides minimum scanning time. The successive chessboard enables to obtain minimum residual stress compared to least heat influence

[66]. Fractal strategies developed for better material properties than conventional island strategy [32]. A consensus has been reached considering the open literature that main importance of the scanning pattern is the effect on residual stress. Residual stresses are effective on surface morphology and quality, especially on surface profiles, and therefore, changing pattern is regarded as an important parameter on the subject of the present review.

In order to determine the scanning time, it is important to study the hatch spacing parameter defined as the distance between two neighbouring tracks. The representation of hatch spacing is shown in Fig. 1. The applied laser beam increases energy density at the determined area, and hatch spacing becomes extremely important as it affects the overlapping region and the proximity of the track. Scanning vectors need to be determined whether overlapping is desired. It is stated from [61] that when hatch spacing is used as doubled, the overlap is also obtained as doubled. It is also reported that melt pool width is not affected by hatch spacing which means partial remelting of the previous track. The most important effect of the hatch spacing is the energy density, and it shows an increasing trend with higher hatch spacing values. Also, with increasing of hatch spacing, hardness value demonstrates decreasing behaviour, according to the authors. Li et al. [23] worked on the densification behaviour and surface roughness considering laser parameters and hatch spacing. It is reported that narrower hatch spacing provides a smoother surface and higher densification along with a series of the parameter. Hu et al. [60] highlighted that hatch spacing depends on scanning speed and affects microhardness. Hatch spacing shows the fluctuating effect on density varying with scanning speed. Huang et al. [59] found that shorter hatch spacing produces lower temperature gradient and higher temperature, affecting residual stress and surface morphology inevitably. Dong et al. [58] investigated the hatch spacing effect on a variety of parameters. It is indicated that with increasing of hatch spacing,

Fig. 4 Scanning pattern strategies
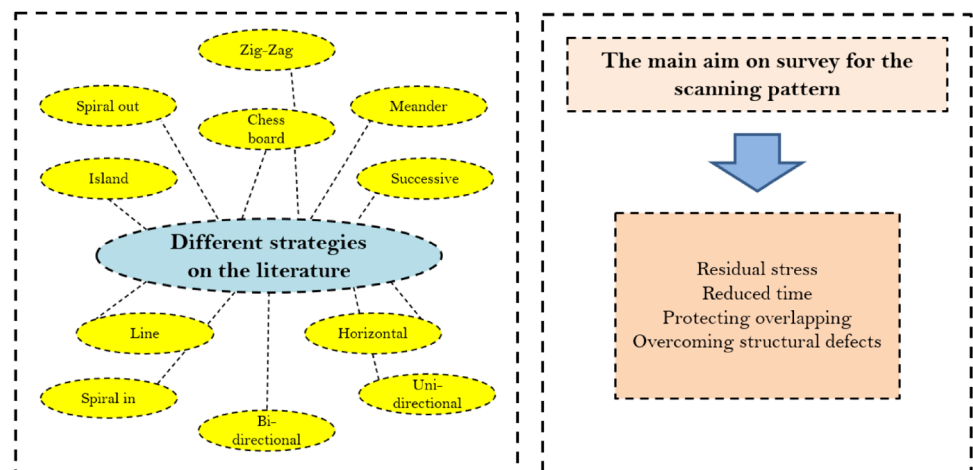
the width of the melt pool decreases, and with an optimized hatch spacing value, the fully dense part can be produced. The review of the literature shows that discriminating hatch spacing from scanning parameters is scarcely conducted, especially in respect of surface morphology. Therefore, more work on the topic is anticipated for better understanding its effect on surface morphology.

2.2.2 Influence of layer rotation angle

The layer rotation angle can be defined as the laser beam angle between two subsequent scanning operations of layers. The basic effect of this parameter is overlapping phenomena due to the influence of rotation angle on the metallic bindings of powders. Therefore, bonds between particles are identified, whether strong and containing voids or pores. Most of the rotation angle examples are examined in detail in the past, such as 0° rotating angle [75], 67° rotating angle [76], 45° rotating angle [64], 15° rotating angle, and 90° rotating angle [65]. Wang et al. [74] found that the metallurgical bonding forces between layers significantly affect it. This is about the filling ability of/about the pores with liquid metal, and good overlap can be achieved. According to Gupta et al. [75], residual stress and surface roughness are reduced with the increase of layer rotation angle. Also, they stated that a direct proportion exists with layer rotation angle between relative density and micro-hardness. Accordingly, the literature review demonstrates a correlation between layer rotation angle parameter and surface morphology indicators. Higher angle values produce low porosity, better powder bonding and thus resulting in good material properties. Scanning strategies have hardly affected the molten pool size, 15° rotate strategy generates lowest stress between line and 90° rotating [65]. A 45° rotate strategy is over in terms of the capability of reducing residual stress compared to horizontal and out-in strategies [64]. Most of the works in literature, reporting the effects of layer rotation, lack evaluation of its feasibility in terms of cost factors and modification requirement in SLM setups. Therefore, it is detected that there is an information necessity on the feasibility of layer rotation angle applications.

2.2.3 Influence of scan vector length

The scan vector length is the laser beam travel distance in producing a line during manufacturing a part with SLM. It can be an intrinsic part of the produced geometry. However, scan vector can be adjusted by means of scan pattern. Scan vector length influences the temperature and longitudinal stress and is measured in terms of the magnitude of the vector. In general, the detection of the effect of scan vector length and direction is carried out with monitoring of the thermal history of the surface. Besides, measurable thermal

gradient increases deposited stress on the surface, creating an anisotropic stress distribution and nonuniform structure on the surface [62]. Kruth et al. stated that the decrease of scan vector length reduces stress [94]. In addition, the application of different scanning vector directions may result in reduced stress [64]. In [79], it is found that the other scan strategy parameters have less influence on longitudinal stress when scan vector length is over 3 mm. It is decided from [78] that 4–6 mm of scan length is more proper for thin-wall parts in order to decrease shrinkage to approximately zero. Scan length is found as responsible for second peak temperature. Among other scanning parameters, the vector length effect was remarked rarely in the past. However, it can be concluded that when considering the residual stress effect on surface morphology, further research is needed to perform.

2.3 Influence of geometric parameters

One of the most influential parameters on surface quality of SLM products is the geometric [95]. Geometric parameters and properties can be discussed under two topics, i.e. layer thickness and surface orientation. In addition to good mechanical properties, surface finish and geometric accuracy are the most covetable requirements [96]. The nature of the SLM method is formation layer by layer formation. This gradual production and its thickness greatly affect the surface quality of the materials [97]. Also, geometric parameters have a significant impact on the mechanical properties depending on the stress distribution. If appropriate geometric parameters are used, the shrinkage mechanism can be restricted by the solidified layers and can cause large residual stresses. The occurrence of residual stress triggers the deviation of the thickness of final products and surface profiles [98].

2.3.1 Influence of layer thickness

The layer thickness is also an important parameter controlling the surface morphology, as shown in Fig. 1. There is a direct relationship between the densification character of the parts and the layer thickness [99]. It is reported that the density of the parts depends on the layer thickness. If the layer thickness is selected as the maximum possible value, the melting and consolidation mechanism between layers is insufficient, and it decreases density [100]. Layer thickness can greatly influence mechanical properties such as hardness, tensile stress, and elongation [81]. As it is shown in the decrease of density, high layer thickness reduces the mechanical properties due to poor bonding quality [101]. Yadroitsev and Smurov [80] conducted a study investigating the relationships between the layer thickness (from 40 to 80 μm) and surface morphology of the parts manufactured from stainless steel 316L powder. The work reveals that

pores become large, regular, oriented, elongated, and perpendicular to the sintering direction if the layer thickness is increased. However, minimal layer thickness causes smooth surfaces owing to fine structure of the sintered trucks. Savalani and Pizarro [81] reported a study that investigates the effects of layer thickness in SLM of magnesium. The layer thickness was decided as 150–300 μm. One of the reasons behind the oxidation mechanism of magnesium products is given as the layer thickness. It is mentioned that the amount of oxidation decreases by approximately 25% as the layer thickness increases. This oxidation–reduction can stem from gradually heating and a lower degree of evaporation. When it comes to surface morphology, while the parts between 150 and 250 μm of layer thickness show flatter surfaces, irregular pores and voids are observed at other parts (higher than 250 μm). Also, surface roughness values (Ra) go up starting from 23 to 29 μm based on layer thickness increase values. In another study [102], Inconel powders are used in SLM method, and effects of layer thickness were determined. Similar to other studies, it is revealed that lower layer thickness values lead to parts, which have good dimensional accuracy and density. In addition, surface roughness (Ra) varies from 3.5 to 12.3 as the layer thickness goes up from 20 to 50 μm. The layer thickness reduces operational time and cost. However, several surface problems occur due to increased layer thickness, as stated by the literature. The topic is convenient for optimization approaches and techniques in respect of surface quality and operational costs.

2.3.2 Influence of surface orientation

Built orientation is another key element that affects the surface morphology and surface roughness of SLM parts. The demonstration of different surface orientations is shown in Fig. 5. Weissmann et al. [82] reported a study investigating the effects of geometric orientation (0°, 45°, 90°) of titanium-based SLM parts. The surface roughness values reveal that the orientation has a great impact on surface quality since the Ra values increase from 1.33 (0°) to 9.83 (90°) μm. Other studies reported that Ra increases from 8 to 14 μm (0–90° orientation) and 8 to 30 μm (0–90° orientation) [103]. The differences between the surface roughness values can stem from shear force which occur temperature gradient between solidifying zones. Due to short consolidation time, there is residual rippling on the surface, and it is shown that this condition can be accepted as one of the main drawbacks of this production method [84]. The authors reported surface values of lateral and top surfaces as 28.587 and 6.384 μm respectively. In another work, the built orientation affects the mechanical properties and fracture modes as well as the surface roughness. However, the differences between elastic modulus and tensile strengths of different oriented parts are not as high as surface roughness values [85]. According to the conducted literature survey, more building orientation works for different alloys seem to be necessary, especially in terms of surface morphology.

2.3.3 Support structure

As an integral part of the SLM method, support structures exist before the final product. Removal of those structures may have surface quality effects. There is a dedicated review on support structures dealing with costs related to the support materials and limited number of available works [104]. According to the literature review, a few gaps have been identified. The most important gap is said to be the lack of a comprehensive method that can significantly reduce the support material while maintaining the mechanical strength

Fig. 5 Demonstration of different surface orientation
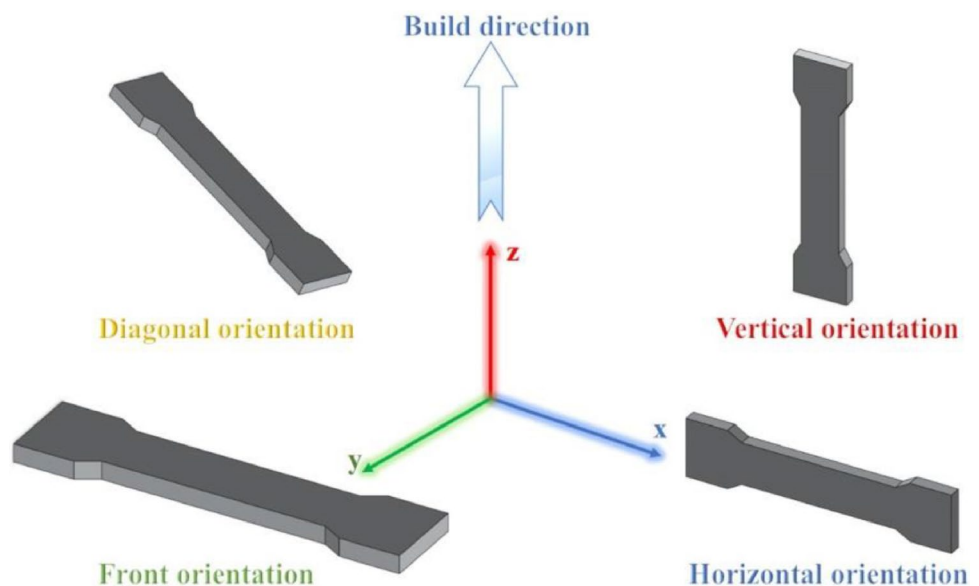
and good surface finish quality. The authors stress the need for developing innovative and creative methods that can largely minimize or even achieve zero-support for AM. As a final remark, they recommended topology optimization techniques adapted by additive manufacturing methods. Günaydın et al. [105] discusses the impact of build orientation on various factors in additive manufacturing, such as part quality, waste amount, production time, and cost. The study presented uses a multi-objective optimization approach with non-dominated sorting genetic algorithm-II to simultaneously optimize different objectives, including the amount of support structure and build time. The developed approach minimizes support structure volume and build time, improving the accessibility and sustainability of the powder bed fusion process. Support structures are also called as lattice structures [106]. For instance, in the cited paper, lattice structure optimization was conducted on a suspension arm to reduce fuel consumption and improve balance in automobiles. Topology optimization was first conducted on the suspension arm to form the model, which was then filled with a lattice structure and re-optimized by size optimization. The results of the study demonstrated the effectiveness of using lattice structural optimization in the design of vehicle elements, as it produced more reliable designs than topology optimization alone, and the configuration and layout of the cellular structures had a significant impact on the overall performance of the lattice structure.

As a final remark on the second section, the authors of the present paper would like to stress out that aforementioned operational parameters of SLM are evaluated by their isolated effects. However, as a general rule of engineering, there may be multiple parameter correlations. For instance, lased power and scanning speed should have a double correlation. Since laser power at a fixed point would only reach steady state by heat transfer balance with environment through radiation, convection and conduction, the heat transfer rate would be lower with passing time in a transient regime. Therefore, scanning speed uses and determines to which extend the heat transfer rate is realized. As a consequence, it is recommended to study multiple correlations of the SLM parameters by future works.

3 Surface morphology enhancement of SLMed metallic alloys

Means for improving the surface quality of SLMed metallic alloys can be divided into three groups, i.e. pre-treatment, post-treatment, and surface machining. Before and during SLM, preparations focus on physical properties depending on temperature and heat transfer mechanisms and process environment. Post-treatment and surface machining are both actually post-processes, but the former one uses heat effects

mostly. Three groups of treatment approaches are identified for the review, as schematically indicated in Fig. 2. Below, these three groups of approaches and methods are given with literature examples. Pre- and post-treatments are also reviewed by Mugwagwa et al. [107] in terms of reducing residual stresses.

3.1 In situ surface improvement techniques

Surface improvement can be achieved by means prior to or in situ SLM. Heating base plate and powders or re-scanning can be applied to improve surface quality. However, in order to decide proper means and precautions, one may utilize other parameters such as the importance of vertical planes, surface roughness prediction, and simultaneous measurement scanning. Yang et al. [50] focused on vertical planes and their implications on surface roughness. The authors emphasized a contrary behaviour of vertical surface roughness. Adhering particles and droplets appear as a problem for vertical orientation. To determine which precautions are needed before the SLM process and during the SLM process also necessitate predicting potential surface roughness values and surface morphologies. Martin et al. [108] report in situ X-ray imaging during SLM processing. They were able to monitor evaporation dynamics simultaneously by the process. Their X-ray imaging technique has ultrahigh speeds for coping with the dynamic mechanisms of the SLM. They reveal vapour depression oscillations. Pores are identified in the proximity of vapour-filled depression bases. Boschetto et al. [109] modelled surface roughness of AlSi10Mg SLMed component. They predict surface roughness after inputting local part geometry as an independent parameter. The staircase effect is accounted for by horizontal and vertical profiles. Still, the model is said to be improved for complex geometries. Vertical surfaces are also emphasized in terms of balling effects.

Surface improvement should also consider the powder morphology and topography since heating base plate and powders have thermal parameters to be previously determined. Powder oxygen content is another parameter that affects surface morphology. Protective atmosphere precautions for SLM processes are contributing and supporting previous thermal operations and re-scanning scenarios. Ferrar et al. [110] investigated several inert gas flow scenarios by numerical analyses. They managed to reduce porosity by 1.7% due to improved gas flow. Although the computational fluid dynamic side of the work can be regarded as weak, the authors overcame this issue with iterative sessions, after which they produced gas flow apparatus (rail) and tested it experimentally. The authors emphasized the importance of gas flow uniformity. One of the essential parameters on the surface morphology of SLMed components is metal vaporization. Dai and Gu [111] investigated

different protective atmospheres in terms of metal vaporization and, accordingly, surface quality. They used a comprehensive numerical model considering various mechanisms, including heat transfer, fluid flow, radiation, and keyhole formation. Investigated protective atmospheres are He, Ar, and N_2. Each one of them resulted in characteristic surface features. The authors explained that heat conduction determines the depth of the pool, while metal evaporation leads to resultant recoil pressure. Ar protective atmosphere provides a stabilization effect on keyhole molten pool fluctuation. Ar protective atmosphere is also found better in terms of surface quality. The authors used Fluent CFD for the numerical investigation. Calta et al. [112] investigated the effects of a protective atmosphere by its pressure and composition. Combining with low energy density, protective atmosphere pressure significantly changes surface morphology. They defined a vapour depression aspect ratio to describe changes. The authors emphasized the boiling temperature of the metal that constitutes melt pool surface temperature, characterizing surface tension and, accordingly, surface quality. They also stressed oxygen partial pressure value. There is also a more recent paper focusing on effect of process atmosphere pressure [113]. Authors utilized numerical methods at powder scale, enabling them to isolate other parameters and focus on sub-atmospheric pressures. Their main outcome is related to keyhole mechanism. As an interesting finding, authors claim that this option increase the stability of keyholes. Cooke et al. [114] present a good review article on the broad perspective of metal additive manufacturing and in situ monitoring is given properly with sufficient examples. Le Dantec et al. [115] explain that balling can occur if the initial oxygen content of powders to be melted by laser is above 0.1 wt%. Authors used in situ imaging for different oxygen content Si powders and investigated tracks after melting. Therefore, powder oxygen content should be inspected and subjected to treatment prior to SLM.

3.1.1 Influence of base plate preheating

Base plate heating is a good way of in situ operation for reducing residual stresses and their derivative disadvantages. Heat is transferred through the base plate to the powder bed, decreasing temperature gradients, and reducing laser density need. However, melt pool size may increase since heat dissipation towards outside of the melt pool would decrease. Mertens et al. [116] investigated base plate heating for 4 different materials, i.e. aluminium 7075 alloy, Hastelloy X, H13 tool steel, and CoCr. Base plate heating is found advantageous though its effect is said to be weaker comparing to laser parameters. Optical microscope comparison of top and side surfaces reveals great improvement in crack patterns and densification. Same base plate heating resulted differently for different materials as expected. The authors

stressed the phase transformation temperature limit for microstructural changes, but they also note that texture can still improve even with higher transformation temperatures.

Borisov et al. [117] focused on base plate heating for SLM building of super alloy Inconel 718 in order to increase production speed. Great heating temperatures are visible in the study up to 900 °C. This temperature of 900 °C base plate heating contributes to the reduction of porosity. Geenen et al. [118] investigate effects on two different base plate heating temperatures on porosity and crack density of SLMed M3:2 high-speed steel. Actually, the authors also compared samples with two other manufacturing techniques, but figures and evaluations specific to base plate heating of SLM appear distinctly. 200 and 300 °C base plate heating temperatures are tested. Low crack and porosity densities are stated to be obtained. Also, some in some instance, cracks are avoided completely by the base plate heating.

3.1.2 Influence of powder preheating

Powder temperatures close to ambient temperature necessitate certain laser energy density (ED) and increases temperature gradients between melt pool and surrounding powder. Therefore, powder preheating may increase production speed and decrease residual stresses. X40CrMoV5-1 steel powder pre-heating is reported by Krell et al. [119]. They subjected powders to five cycles in total. They determined powder densification. The authors tried to achieve the best powder flowability before pre-heating. The microstructure is not affected by pre-heating, but porosity and crack densities show improvement. Tillmann et al. [120] attributed surface tribological behaviour due to austenite content to 200 °C pre-heating. Sochalski-Kolbus et al. [121] state that powder pre-heating, which is an intrinsic part of their electron beam melting, discriminates samples from SLMed samples due to smaller residual stress values, which in turn improves surface quality. Doubenskaia et al. [122] also heated powders. Powder preheating is explained as lowering residual stresses. Together with manufacturing environment preheating, powder preheating resulted in a homogenous micro-hardness at the surface. However, surface cracks and porosity seem unaffected. The leading cause of porosity is determined as evaporating aluminium in the alloy. Rombouts et al. [123] explain that powder preheating in combination with small scan spacing reduces spherical gas inclusion in iron based SLMed components. Authors preheated Fe–C powders and also found positive effects on density. Powder preheating becomes a necessity where meting point of the material or alloy and temperature resistance are relatively high, and thermal conductivity is low. An exceptional instance to this paper is SLM ceramic case, which can be regarded as an exemplifying instance to the phenomenon (Fig. 6) [124]. Extreme powder preheating temperatures are apparent in

Fig. 6 An exceptional ceramic SLM example in order to emphasize effect of powder preheating on densification and crack avoidance [124]
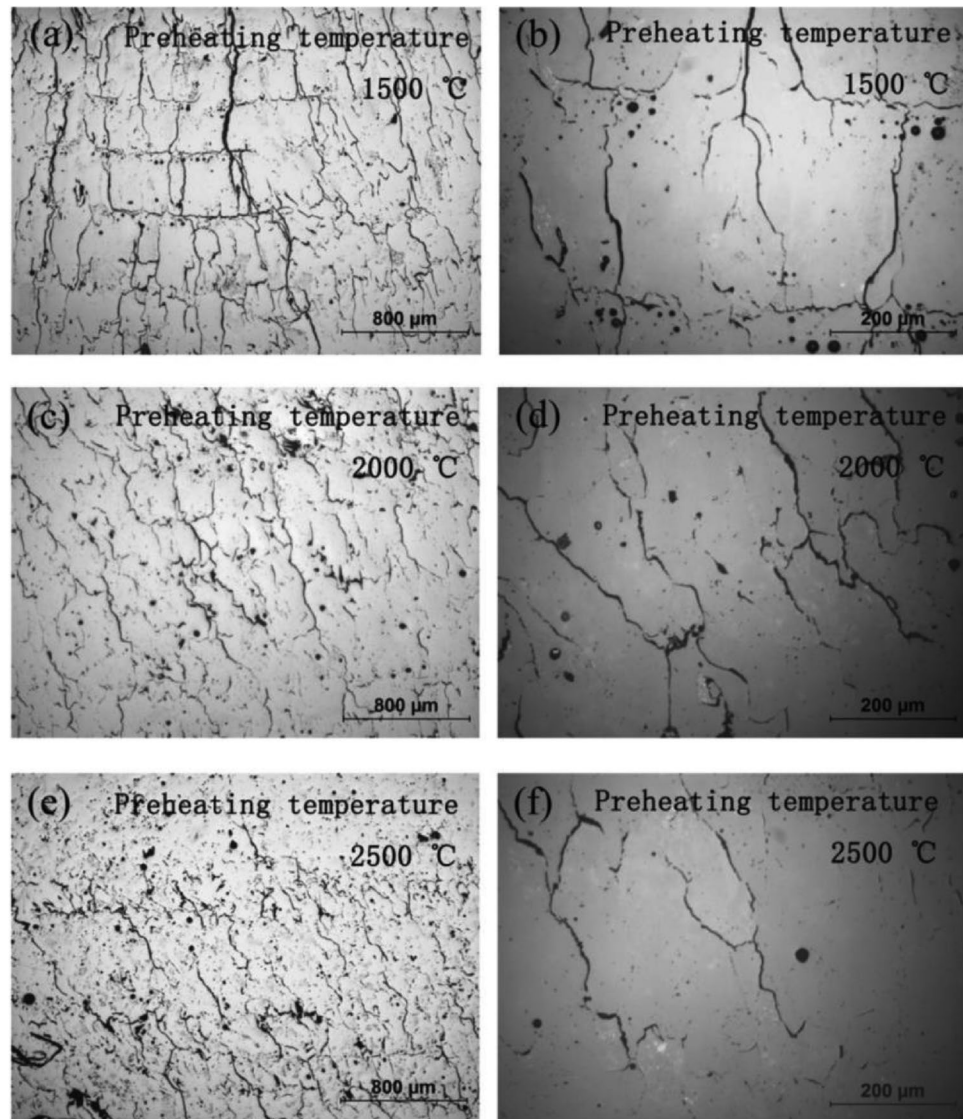
the work of the authors. The powder preheating treatment reduces crack formation and prohibits propagation of the cracks. This also leads to higher sample densities. Therefore, authors regard powder preheating as the only effective tool for the low thermal conductivity and high melting point case.

Domashenkov et al. [125] applied 600 °C preheating to NiTi powder in order to reduce thermal gradients. However, powder preheating triggers high-temperature oxidation and increases the cracking of the re-melted powder. Li et al. [126] report the insignificant effect of powder preheating for TiN reinforced Al12Si in terms of relative density compared with the effect of laser focus. An exciting and rare work reveals the energy consumption aspect of powder preheating [127]. Authors claim that up to 40% of the total energy consumption of SLM can be due to powder preheating. Although a portion of that energy can be attributed to base

plate heating, a considerable portion belongs to the powder preheating. Especially pre-scanning not only contributes to energy cost but also increase the production time. Authors utilized numerical analysis by finite elements method. Another important condition that is given by the authors is that preheating strategy should be selected according to SLMed part number since low numbers may be done best with laser pre-scanning while high numbers make ambient heating favourable. Surface distortion is reduced about 45% and relative density is increased about 3% by preheating Ti6Al4V powder up to 550 °C in the study of Malý et al. [128]. The authors warn that powder preheating degrades chemical status by excess hydrogen and oxygen content which in turn pose a limit for its usage in some applications. On the other hand, Mertens et al. [129] tried four different powder bed preheating from 100 to 400 °C for H13 tool steel, and they reported a stress conversion on the top

surface from compressive to tensile. Alongside with better mechanical properties due to powder preheating, the authors do not state any adverse effects.

3.1.3 *Influence of* in situ *re-scanning*

Re-scanning is a good strategy to relieve residual stresses and improve surface quality. However, it may increase production time and costs. Also, re-scanning parameters should be carefully determined in order to prevent adverse effects. Additionally, re-melting a solid layer may lead to faster cooling and therefore crack formations. Pal et al. [8] compared SLMed Ti6Al4V samples with samples that are subjected to re-scanning. The re-scanning was realized by applying a low-density laser and consequently re-scanning with proper laser power again. While authors stressed the unpredictability of surface morphology due to many laser processing parameters, significant changes are reported. They applied different laser processing combinations for re-scanning and detected very different surface morphology results. One of the major problems that are associated with re-scanning is the balling effect on vertical surfaces. Adhered powder particles are visible and numerous in vertical surface morphology. Nevertheless, re-scanned top surface defects have similarities with single SLM scans, i.e. pores, spherical spattered particles, and stacked materials. Again, the two main creator factors of defects due to re-scanning seem to be low laser ED and high scanning speeds. Yasa et al. [130] investigated re-scanning in order to improve the surface quality of SLM. An excellent surface improvement on the horizontal upper surface is visible by relatively slow re-scanning. The authors also claim that re-scanning increases surface density or shell density. Another interesting point that is addressed by the authors is the easier machining possibility of re-scanned surfaces. Griffiths et al. [131] evaluate their re-scanning strategy considering the work of Yasa et al.

[130] in terms of surface smoothing and changed melt pool shape due to the re-melting. The authors explain that columnar grains are replaced with equiaxed grains after third re-melting since the second re-scan leads to smoother surfaces which in turn reduces absorptivity and hence leads to shallower pools (Fig. 7). A comprehensive review of Aboulkhair et al. [132] gives an illustrative example of scanning strategies. Pre-sintering with a low ED laser and subsequent re-scanning seems to give the best surface results. Xiao et al. [133] investigated multiple re-scanning and stated that relative density first increases and then decreases by increasing the number of re-scans. However, the study lacks in terms of surface metrics. A different re-scan strategy with applying high ED laser first and then re-scan with low ED laser in order to relieve high residual stresses by Li et al. [134]. The authors stressed a good surface finish in the absence of macro-cracks.

Chen et al. [88] mark overlap regions of scanning as a way of re-scan for residual stress reduction. However, the authors state that this strategy is inversely affecting if too much overlapping is done. This adverse effect of overlapping after the limit value is attributed to the reducing pre-heating effect of the scanning for the next hatch. The authors also tried vertical re-scanning with a short scanning length to reduce residual stresses further. It should be noted that the authors utilized numerical analysis. Ali et al. [73] reported adverse effects of re-scanning on Ti6Al4V SLMed alloys. Authors tried varying re-scan laser density and exposure times; however, residual stresses are not reduced significantly, and more porosity is observed. According to re-scanning, a major study about surface evaluation of SLMed AlSi10Mg is reported by Yu et al. [4]. Authors focus on the surface roughness of vertical and horizontal surfaces and also evaluate pore structures. They managed to reduce surface roughness twofold by re-scanning. However, re-scanning increased the surface roughness of the side surfaces.

Fig. 7 Modification of the melt pool by re-scanning [131]
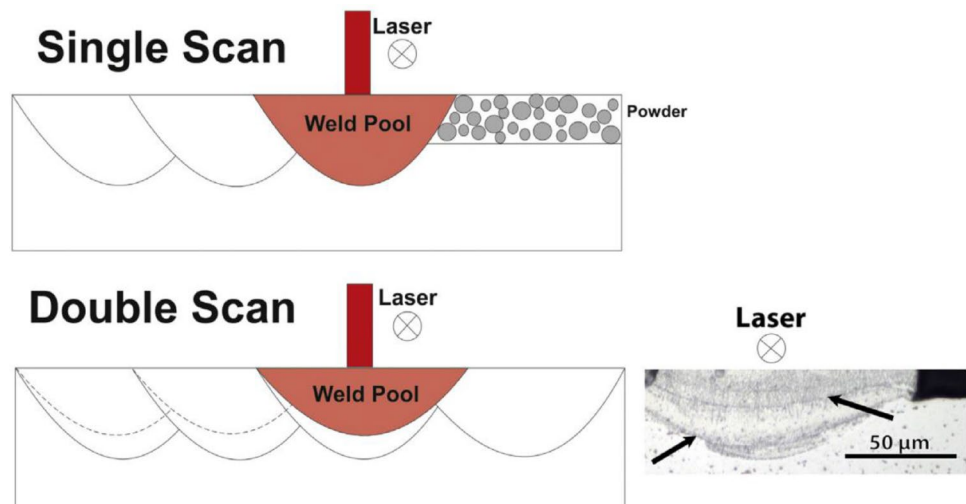
They explain pore-creating mechanisms. Re-scanning is emphasized significantly reducing irregular pores that are mostly due to lack of fusion. As a major conclusion, they recommend same re-scan direction with the first scan in order to reduce pores at the track sides since the same direction scan and opposite direction scan result in almost the same pore improvement at central locations on the track. Miao et al. [135] used experimental and numerical means to analyse the effects of three different re-scanning strategies on Ti6Al4V. Authors' detected residual stress are reduced from 322 to 254 MPa. Optic microscope results of the work also show differences in single and re-scanned surfaces.

3.2 Post-processing techniques

Post-processing of SLMed parts mainly focuses on heat treatment. However, there are methods relying on different physics for better surface morphology and quality. Heat treatment does not seem directly related to the surface. Maleki et al. [136] propose three groups, i.e. "no material removing (NMR)", "coating", and "hybrids". It is also worth mentioning that the authors' paper is a good and organized reference for post-processing techniques. However, the authors consider all metal additive manufacturing (AM) methods. NMR includes rolling, bead blasting, shot and cavitation peening, ultrasonic nano-crystal surface modification under mechanical approaches. There are also laser-based approaches that consist of laser shock peening, laser re-melting, and laser polishing. Several coating strategies can be listed as electro-spark deposition, electro-phoretic deposition, hydroxyapatite coating, anodizing, and plasma electrolytic oxidation. Hybrid approaches combine coating, heat, and mechanic methods. Polishing is excluded from machining and regarded as a "quasi"-no material removing method. In that case, there are polishing options such as mechanical, magnetically driven abrasive, hydrodynamic cavitation abrasive, and ultrasonic cavitation abrasive polishing methods [136]. Selecting the proper method depends mostly on the material and the application that the SLMed part is to be used. However, it can be easily stated that surface roughness is greatly reduced (up to tenfold) by polishing. If the surface is convenient in terms of plastic deformation, mechanical means are used to shape the surface. Also, the thickness of the SLMed part is favourably modified. However, perpendicular surfaces may be negatively affected. Mechanical abrasion can remove surface oxides and contaminants. Shot peening and bead blasting can be given as examples. Shot peening and bead blasting can also increase surface hardness. However, the shot peening method may lead to rougher surfaces than bead blasting. If shot action and blasting solids are somehow undesired, cavitation can be utilized as a way of impacting the surface. The cavitation phenomenon is known as an instant forming

and collapsing bubble in a fluid. The collapse of bubbles leads to an instant and dramatic increase in pressure acting on the local surface. Cavitation peening can also be combined with a cavitation jet. Considering the impact effects of peening techniques, one should decide the proper one by the brittleness of the surface due to its material and mechanical properties. Although there are studies comparing peening techniques, the reasons and underlying physics for results are rarely apparent [136].

3.2.1 Influence of heat treatments

Lizzul et al. [137] used heat treatment before machining SLMed prisms in order to stabilize microstructure and reduce porosity and thermal stresses. An argon atmosphere was used for 30 min to apply 950 °C temperatures on Ti6Al4V SLMed parts. It is also worth noting that ramp-up time was 2.5 h. They used 20 bar argon flow for cooling. However, no direct implications of the heat treatment on the surface are stated. Cooke et al.'s [114] review reveals numerous works utilizing heat treatment as post-processing. However, there is no sign of a significant effect on surface roughness and morphology. Fifty percent of reviewed works about post-treatments of the authors' are on heat treatment, and most of the improvements of SLMed parts are related to grain size and mechanical properties of subsurface structure. Alghamdi et al. [138] tried post-fabrication heat treatment with 1 h solution heat treatment at 520 °C for AlSi10Mg and then tried three different cooling strategies, namely water quenching, air cooling, and furnace cooling. However, texture and morphology results are mostly related to structures of columnar grains. Although Geenen et al. [118] have examinations on the surface for cracks and pores, they do not correlate their heat treatment with surface quality. The review of Aboulkhair et al. [132] also does not reveal any aspects of surface morphology relating to heat treatments though numerous papers are reviewed in terms of heat treatment of SLMed aluminium alloys. Krell et al. [119] applied 1040 °C to X40CrMoV5-1 for 30 min and then applied oil quenching. After two hours of tempering furnace and air cooling, the hardness of the material is stated to be positively affected. No direct information is given on surface morphology related to the heat treatments. Several other papers report heat treatments of SLMed parts [37, 85, 139–141]; however, a significant relationship between surface morphology has not been encountered.

3.2.2 Influence of peening techniques

Peening is a good alternative in post-processing of SLMed parts for good surface morphology properties if the SLMed part does not have a very complex and compact internal surface and does have properties adequate for plastic

deformation on the surface. Cooke et al. [114] mention peening in their review about metal AM. Authors denote peening as a relatively conventional method that can provide surface roughness reduction up to 30 μm. Residual stresses on SLMed AlSi10Mg are treated by using shot peening in the study of Salmi et al. [142]. Authors state that peening relieves high tensile stresses of as build parts as a post-processing approach. The instrument is given as NORBLAST SD9 shot-peening machine. The machine uses 3 bar pressure, zirconia beads having 200 μm diameters, and a 45° shot angle setup. Authors claim that shot-peening not only converts stress type but also provides uniformity. Benedetti et al. [143] combined shot-peening with tribofinishing in order to have good surface roughness and fatigue resistance. Authors propose shot-peening as a tool that provides not only improvement surface roughness but also an increase in fatigue resistance. A comparison between as build parts, shot-peening, and other two methods is given in Fig. 8. In the figure, tribofinishing, a technique that polishes the surface by a bath of solid abrasive spherical particles, is also presented.

3.2.3 Influence of polishing techniques (electrochemical polishing, mechanical polishing)

Polishing is and old and well-known technique for surface morphology–related phenomena. A schematical representation of two different polishing approaches is given in Fig. 9.

On the other hand, a state-of-the-art engineering possesses numerous polishing techniques different from conventional ones. A great example of chemical polishing is given by Soro et al. [144] on titanium lattices. Lattices are very compact in terms of their surface area divided by their volume. This type of compactness and subsequent internal surfaces eliminate most of the polishing methods as being options. Chemical polishing is a great tool in such a condition, as it can be observed in the work of Soro et al. [144]. Three types of Ti6Al4V lattice structures were subjected to chemical polishing. The authors investigated polishing time as they tried several different intervals. Powder residuals adhered to the surfaces was effectively removed, and stair shapes were eliminated. Soro et al. [144] are given in order to show their schematic chemical polishing technique and a result of it. However, it should be mentioned that chemical polishing may lead to weakened struts after a certain amount of polishing time for especially Schwartz's primitive geometry.

Cooke et al. [114] addressed electrolytic and laser polishing methods for SLMed parts. Especially, electrolytic polishing seems to be the only alternative to chemical polishing for SLMed parts with compact and complex internal structures such as lattices. Laser polishing provides flexibility since the laser can be applied with a lot of different axes. Cooke et al. [114] also stress that the Ar environment eliminates oxide formations when laser polishing is preferred. Zhang et al. [145] investigated the electropolishing mechanism of SLMed Ti6Al4V. Two electrolytes were used, i.e. glacial

Fig. 8 **a** As build, **b** tribofinished, **c** electropolished, and **d** shot-peened [143]
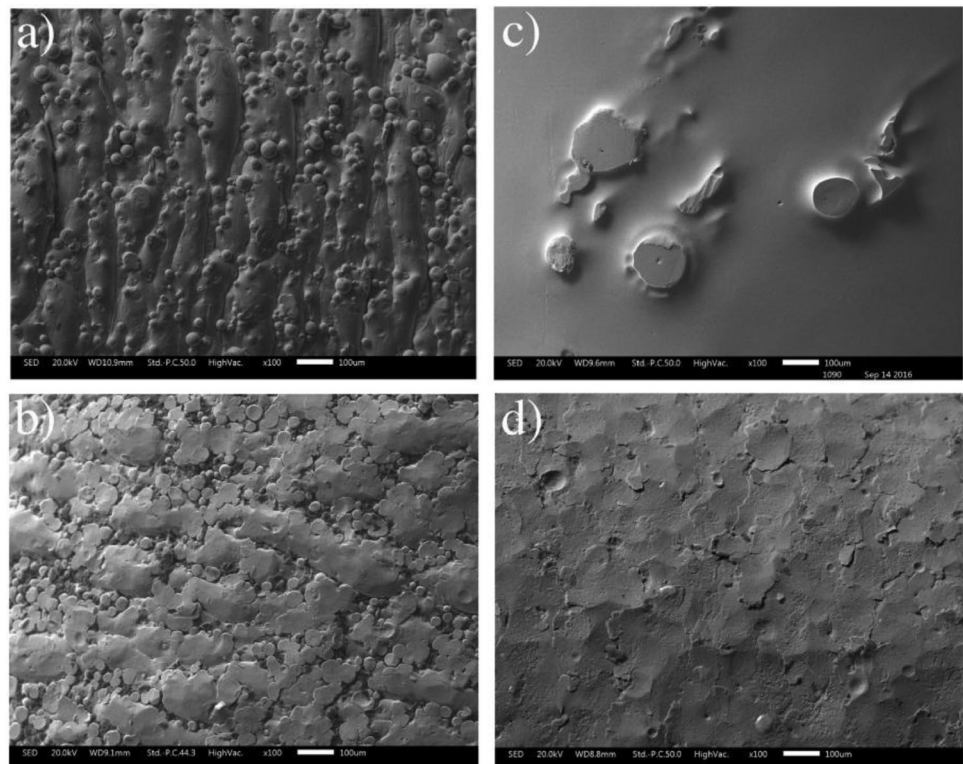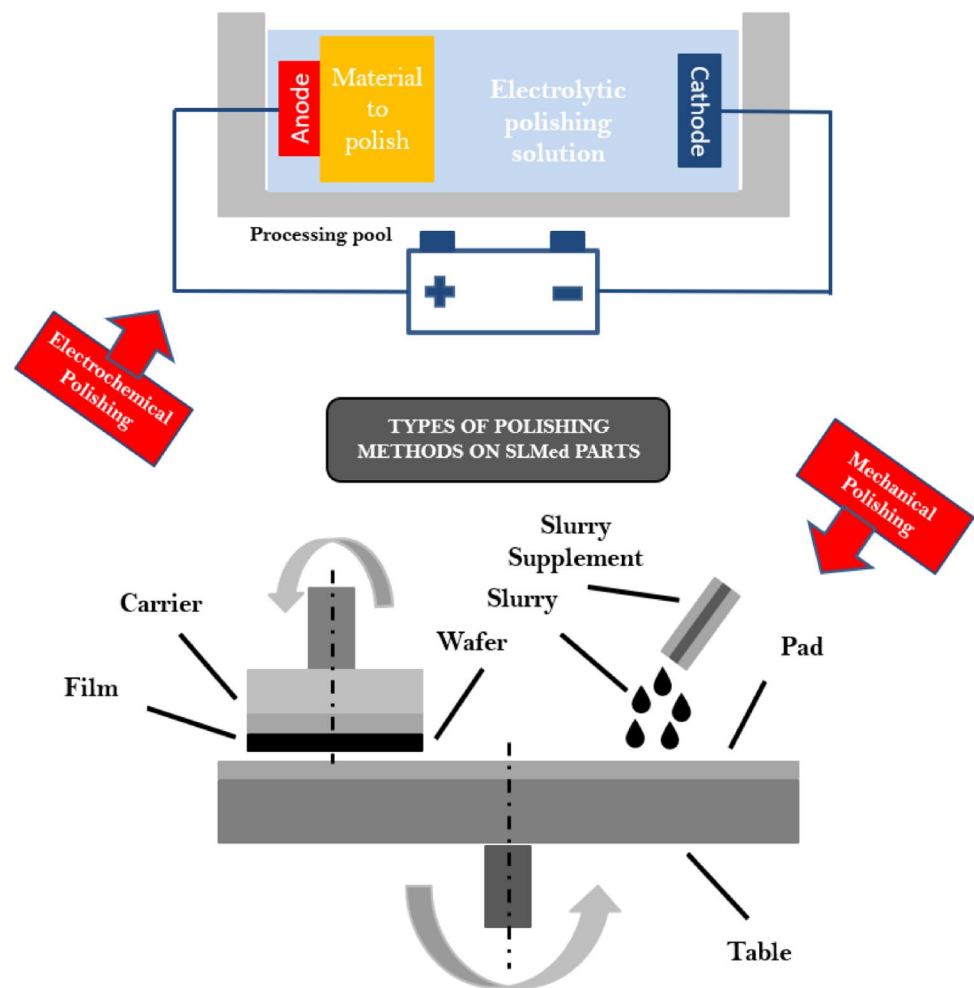
Fig. 9 Polishing techniques used for SLMed parts

acetic acid and perchloric acid. Their results in terms of surface morphology show that three types of oxides cover the surface containing vanadium, titanium, and aluminium oxides. That is, of course, expected due to the composition of the alloy. The authors recommend 15 min polishing time for the ideal surface quality. Additionally, increasing corrosion resistance by prolonging polishing time is reported [145]. Benedetti et al. [143] also used electropolishing. However, the authors state that electropolishing may lead to crack initiation site under the surface due to the influence of the method through pores. Plasma electrolytic oxidation for bio functionalization of SLMed Ti6Al4V is reported by van Hengel et al. [146], that is a data article showing the time-dependent change in surface morphology. Three images are given for 300 s with 200-, 500-, and 1000-fold scanning electron microscope (SEM) images are visible in that report.

3.3 Finishing with machining

Surface finishing of SLMed parts with relatively more conventional methods has always been an option for better surface morphology and quality. Especially external surfaces of SLMed parts are favourable in terms of conventional finishing. Therefore, this review subsection is held relatively short comparing to other parts of the paper. Nevertheless, there are on-going efforts for certain aspects of machining techniques towards SLMed parts. There are also newly emerging approaches that are to be introduced in this part. Relatively more bulk material removal is intended with machining, unlike polishing techniques. Nevertheless, the intrinsic structure of SLMed parts due to its layered shapes and micro-defects may lead to different effects on surfaces. Therefore, there are several papers on the surface investigation of machined finishing of SLMed parts. The review of Maleki et al. [136] only mentions milling and grinding processes. They emphasize successful reduction of surface roughness and improvement of fatigue performance. Surface machining has the role of decreasing residual tension stresses on the surface since some amount of material is removed from the surface. Surface roughness can be reduced at a rate of 90%, and fatigue strength improvement up to 50% is given as an example [136]. It is also noteworthy to state that there are different means of employing water jet and electrical discharges. Similar to other post-treating methods,
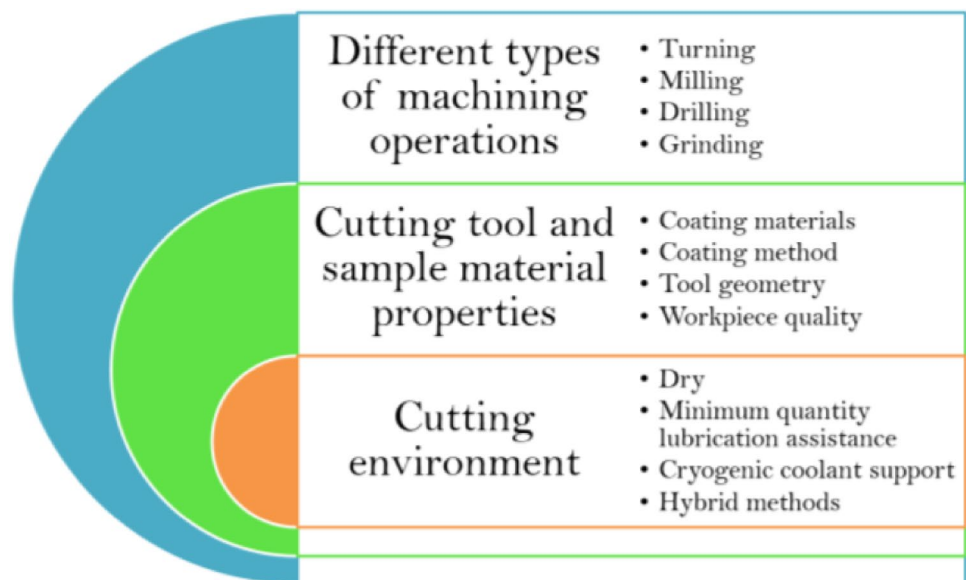
machining induces additional time and money costs to SLM. Accordingly, decision-making on machining SLMed parts does depend on not only machining performance but also specifications and needs of the industrial application. On the other hand, surface metrics, especially surface profile, of machining have characteristic features such as ordered surface tracks and shapes. Yet, surface evaluations related to the machined surfaces are well established in the literature.

3.3.1 Influence of mechanical machining

Mechanical machining methods such as milling and grinding are favourable when relatively flatter external (top and sides) are considered. At geometrical conveniency available conditions, conventional mechanical machining that has several elements, as are shown in Fig. 10, is very powerful and cost-efficient. As mentioned, elements in Fig. 10 are discussed in the following, recent examples from the literature are cited. Lizzul et al. [137] investigated the interaction between the building orientation of SLMed samples with slot milling parameters in terms of surface topography. Authors provide 3D surface topography graphics of milled surfaces. They identify adhered elemental chips, adhered micro-particles, and smeared feed marks on the milled surfaces. The material was Ti6Al4V. SLM-induced anisotropy is given as the main reason for surface defects after milling. Several parametric results are explained in detail by their interaction leading to the surface results. Yang et al. [147] also identify feed marks, smeared materials, and adhered particles on the surface of milled SLMed Inconel 625. They correlated building orientation, scanning direction, and relative milling orientation for identified surface defects. High anisotropy of SLMed Ti6Al4V alloy is investigated in conjunction with milling for

surface morphology by Ni et al. [148]. Authors also report better surface quality based on surface alignment and scanning orientation. Khaliq et al. [149] studied micro-milling of SLMed Ti6Al4V under dry and "minimum quality lubrication" conditions and report surface quality. The main aspect of the work, however, is tool wear. Nevertheless, a surface roughness value below 0.6 μm is given. Cooke et al. [114] and Vaithilingam et al. [150] include mechanical polishing surface treatments as machining techniques. Nicoletto et al. [139] used surface machining for one heat-treated sample in their work. By this way, they managed to define a 0.3 fatigue as-build surface knock-down factor. Siddique et al. [151] report approximately a fivefold surface roughness decrease by mechanical machining. Edwards and Ramulu [152] utilized mechanical machining for T-bone samples of SLMed Ti6Al4V. Photographs of the machined and as-built samples enable qualitative comparison of their surfaces. Brandl et al. [153] machined 91 samples of SLMed AlSi10Mg. Several other factors were investigated alongside of machining, and statistical analyses alongside with Weibull distribution were conducted. They used machining for removing residual stresses, distortions, and contaminations. Al-Rubaie et al. focused on machinability of as build and stress relieved SLMed parts for toroidal milling process [154]. Although they focus on general machinability, the authors provide surface roughness values of toroidal milled SLMed as build and stress relieved samples, alongside surface profile results. Additionally, it is stated that SLMed toroidal machinability is found better comparing to conventionally build sample. Yasa et al. [130] examined micro-machining capability of SLMed parts. Inner and outer features with 50–100 μm are identified for micro-machining capability. Didier et al. brought the idea of using SLM technology to manufacturing

Fig. 10 Several aspects of the mechanical machining processes affecting the part quality

Different types of machining operations
- Turning
- Milling
- Drilling
- Grinding

Cutting tool and sample material properties
- Coating materials
- Coating method
- Tool geometry
- Workpiece quality

Cutting environment
- Dry
- Minimum quantity lubrication assistance
- Cryogenic coolant support
- Hybrid methods

supports for milling thin metal sheets [155]. Authors tested this idea by producing supports and the thin metal sheet by SLM. They utilized confocal microscopy and presented surface profiles of cut and rough portions.

It is inferred that the main problem associated with machining SLMed parts, in terms of surface morphology and quality, is the anisotropic and uneven surface distribution before machining the surface due to the SLM method. This leads to insufficient or over machining local domains and regions on the surface. An adaptive tool track, supported with visual scanners for local morphology determination can be regarded as a future research subject.

3.3.2 Influence of water jet machining

Water jet provides coordinate system flexibility, resembling laser techniques, and can reach more complex surfaces, even internal and ground facing ones. Since water jet has relatively less temperature rising impact than other cutting methods such as laser or mechanical cutting, its thermal effects are expected to be relatively low. Nagalingam and Yeo [156] utilized a multi-jet approach for surface finishing of Inconel 625 SLMed alloy. They tried their hydrodynamic machining approach on different diameter channels with different surface topologies such as stepped or linear. With 15 min application of abrasive particles having less than 1% concentration resulted in surface roughness reduction between 60 and 90%. The work is very comprehensive and informative. Nagalingam et al. [157] also used the same technique for the SLMed fuel injector and applied abrasive flow for the surface finish of internal surfaces.

Although the literature is surveyed comprehensively, there is no other work on water jet machining of SLMed parts to the authors' best knowledge. However, abrasive flow works are given below due to its resemblance in fluid utilization. Nagarajan et al. [158] compares surface machining techniques for favourable surface morphology of SLMed parts and only mentions one study about water jet abrasive surface finishing. That mentioned work belongs to Wang et al. [159]. They applied abrasive flow (AFM) machining to internal and external surfaces of aluminium and titanium SLMed parts. They emphasize its flexibility for difficult to access surfaces. Guo et al. [160] used a similar AFM technique for the surface quality of internal surfaces. They used SLM Inconel 718. El Hassanin et al. [161] assisted AFM with rotation. For SLMed AlSi10Mg alloy, they obtained slightly better surface roughness. Balyakin and Goncharov [162] designed a hydro abrasive unit for SLM and analysed it by CFD. Then, they tested their design experimentally and investigated several application periods. A 15-min application is suggested due to its surface results. Gilmore [163] stated that lattice structures of SLMed 316L might be regarded too complex for AFM. Han et al. also worked with

AFM regarding internal channels of SLMed parts; however, their main focus was on fatigue phenomenon [164]. Yet, the work presents great information about surface morphology by surface profiles and topographies. Especially, the visual quantitative and qualitative comparison of an internal passage, treated with wire electrical discharge machining (EDM) and with AFM on separate samples, provides unique assessment opportunities, and accordingly, an example of their comparison is given in Fig. 11.

3.3.3 Influence of wire EDM

Wire electrical discharge machining (EDM) is a method in which cutting is done with a line tool. This line passes throughout the part to be machined. Therefore, characteristic geometries necessitate this technique. Guo et al. [165] compared wire EDM with grinding and milling for machining of CoCrFeMnNi high-entropy alloy. The authors provide a great visual comparison between EDM and mechanical machined surfaces. Surface morphology and roughness aspects are laid out. EDM eliminates tool marks of the grinding and milling. Golubeva et al. [166] investigated the usability of SLM on residual powders of EDM. The material is a Ni-20Cr-10Fe-3Ti heat-resistant alloy. However, poor surfaces are visible after SLM. Fette et al. [167] used EDM for surface finishing of SLMed molds. Authors suggest EDM and milling for a better surface due to usage requirements of the parts. Rickenbacher et al. [168] include EDM of SLMed parts as a cost parameter in their work for developing a general SLM cost model. Hassanin et al. [169] used micro-EDM for surface finishing of SLMed Ti6Al4V parts. Authors provide qualitative comparison photographs of as-build and EDM surfaces. EDM parameters are revealed in work with detail. As given in previous subsection, Han et al. used EDM in order to improving surface of an internal channel from a SLMed part [164]. Authors suggest EDM as a reference method to compare with AFM. This is evidence that EDM's reliability for SLM surfaces, especially for internal channels. Both EDM and AFM methods are claimed to increase the fatigue performance of the SLMed parts by improving internal channel surface morphology.

Zhao et al. [170] introduce a new way of using electrochemical means to remove adhesive powders from SLMed part internal surfaces. Authors describe a flexible cathode in order to reach internal holes. They reached to approximately 50% reduction in the surface roughness of the hole. They also tried reciprocation the flexible cathode for a curved hole and obtained favourable results. The main targets on the hole internal surfaces are given as adhered powders and band protrusions. Their flexible cathode with reciprocating movement is schematically given in Fig. 12. Same authors, in another paper, modified the flexible cathode and formed

Fig. 11 Comparison of surface topographies of three internal channels; **a** SLM + EDM, **b** as build SLM; **c** SLM + AFM [164]
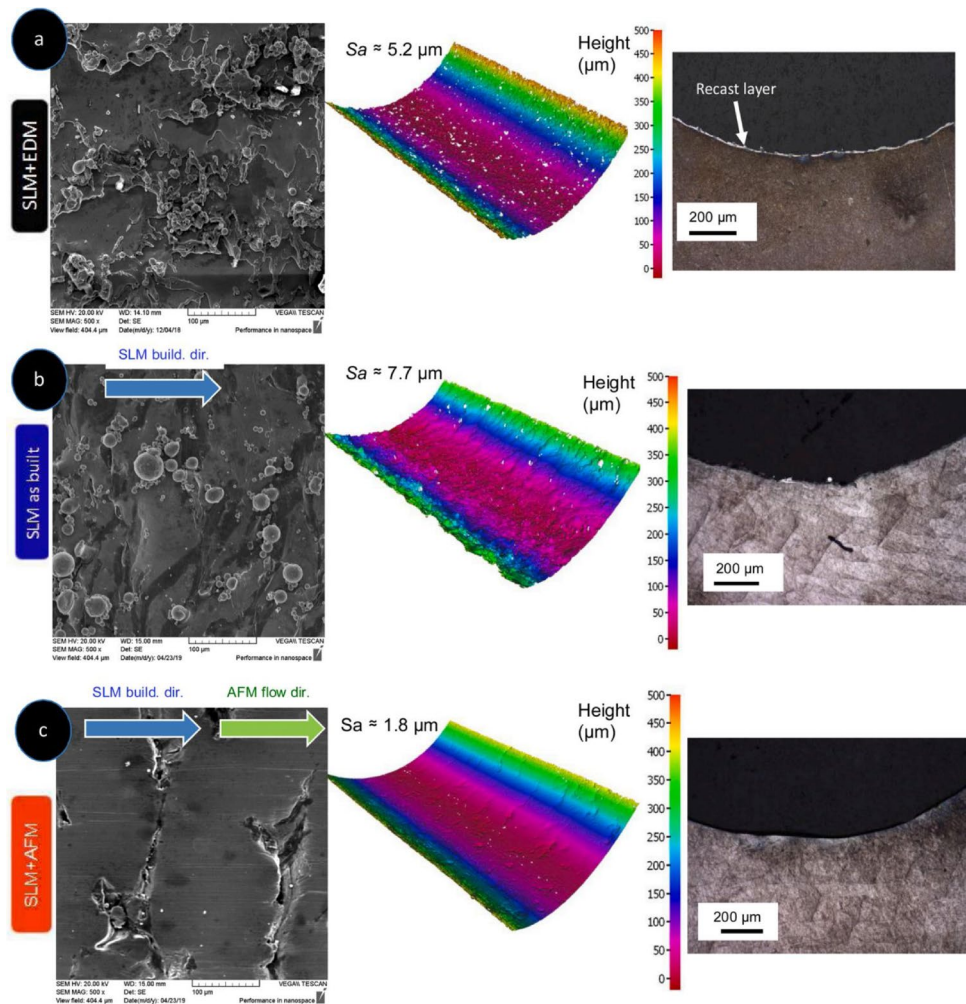
a "brush" in order to increase and support the physical process with mechanical interference [171]. They denominated the approach as electrochemical mechanical polishing. Smoother surfaces alongside with fewer pores thanks to the mechanical interference were claimed by the authors.

3.4 A general assessment of reviewed surface morphology enhancement methods of SLMed parts

According to the review of pre- and post-processes for treating surfaces, Table 3 is composed in order to classify approaches considering their offerings. This table is composed based on qualitative evaluations on the literature and perception of the authors of the present paper. It is very hard, if not impossible, to create a solid and quantitative universal scale due to the broad range of research, great variety of all kinds of independent and dependent factors, and availability of data. We recommend the reader to view the table as a

summarized quantitative understanding and assessment of the authors of the present paper.

Green colour in Table 3 indicates favourableness, and red colour shows ineffectiveness while grey poses a moderate effect. According to Table 3, laser re-scanning, peening, and polishing seem to be very effective methods. However, they induce more time and operational costs. Base plate heating, on the other hand, is an in situ operation with relatively ignorable costs. Most of the cost evaluations in the literature state qualitative assessments. A universal measure and a non-dimensioned procedure are necessary.

4 Surface morphology–induced variations in the behaviour of SLM components

Significant benefits and enhancements can be obtained by viewing and controlling surface morphology-induced variations in SLM components' behaviour during the manufacturing process. The property estimation of SLM components depends on various parameters such as geometric

Fig. 12 A flexible cathode for electrochemical machining of a curved internal surface [170]
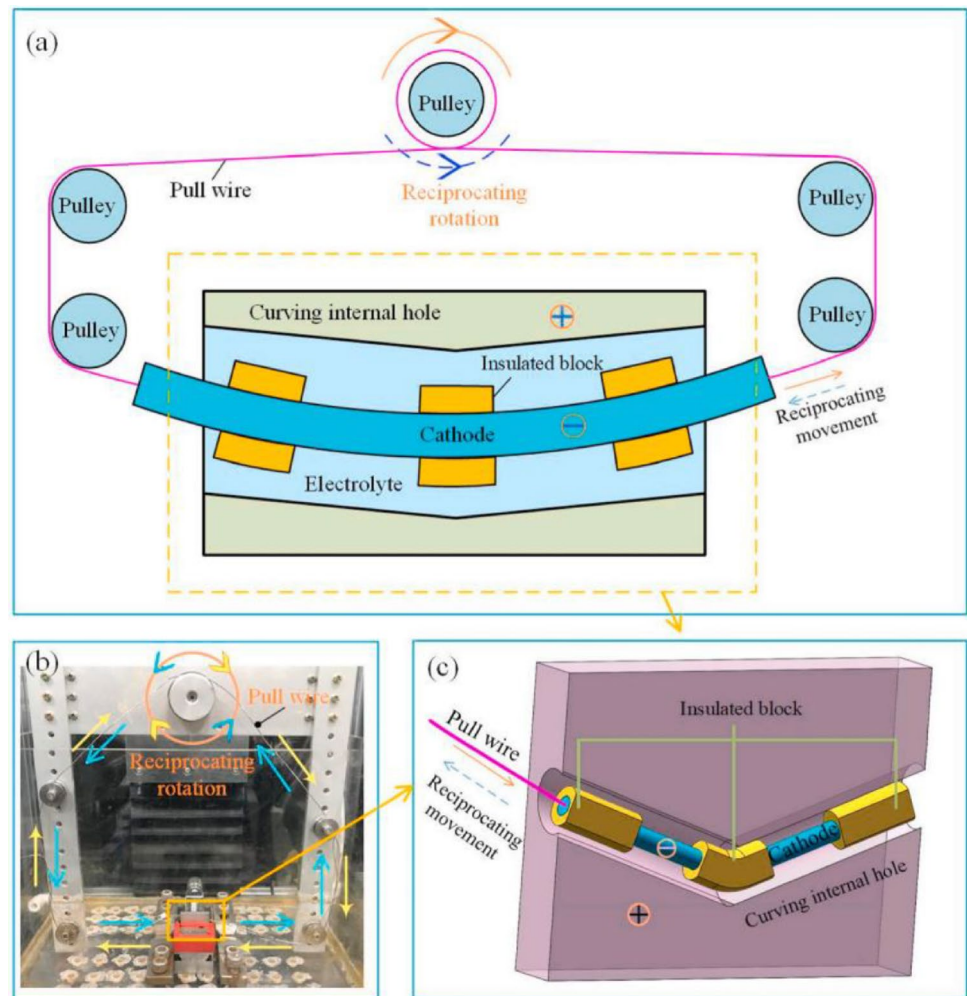
characteristics, fatigue behaviour, surface quality/morphology, density, and mechanical properties of materials in addition to low costs and high productivity. Recent research from literature is reviewed to comprehend how surface morphology–induced variations' effects on SLM components behaviours.

4.1 Fatigue behaviour of SLM components

Structural variations stemmed from chemical composition changes, shrinkage voids, porosity in the SLM layers, vicinity of cavities, surface morphology, and other metallurgical defects directly or indirectly manipulate SLM components' fatigue behaviour similar to the fatigue characteristics of traditional powder metallurgy produced components [176]. These behaviours are not yet comprehended thoroughly because various parameters and their correlations exhibit distinctive effects on end SLM products' properties. Therefore, estimating and controlling the end product properties can become a challenging issue for manufacturers and researchers. Some studies have been conducted on surface

morphology-induced variations, which are among the most influential parameters on the fatigue behaviour of SLM components [177]. Surface morphology-induced variations are compromising mainly porosity, surface roughness, and residual stresses. Since crack initiation occurs in the structure because of porosity, surface quality, residual stresses, specific microstructures, and their combinational effects, researchers have arduous to measure and understand these variations. The residual stresses can be removed by systematic intervention to SLM parts, and fatigue strength can be increased by reducing structural defects, particularly internal defects, with the subsequent heat treatment. Although the SLM components' defects are reduced or eliminated by closing the pores with stress relieving and hot isostatic pressing processes, the surface quality and other surface-related defects continue to be problems that need to be addressed. Although the surface quality is improved by chemical etching or tribofinishing processes, the application areas of these processes are limited. One of the reasons is hazardous etching agents. They release toxic gases to environment. Besides, the tribofinishing process is not

Table 3 Effectiveness evaluation of pre- and post-treatments in terms of surface

	Surface Roughness	Residual Stresses	Porosity	Surface Cracks	Surface Morphology (Profile)	Ball Forming	Spatter Residuals	General Cost
Powder pre-heating	Insignificant (self-evaluation)	Very Effective[119, 121, 122, 129]	Effective[119, 122, 123, 126]	Effective[119, 122, 125]	Effective[120, 128]	Effective (self-evaluation)	Effective (self-evaluation)	Low[127]
Base Plate Heating	Insignificant[122]	Very Effective[172, 173]	Very Effective [116-118, 151, 174]	Very Effective [116, 118, 151, 174]	Effective [122, 175]	Effective (self-evaluation)	Effective (self-evaluation)	Low (self-evaluation)
Laser Rescanning	Effective[4, 131, 134]	Very Effective[8, 73, 88, 134, 135]	Very Effective [4, 8, 73, 130, 133, 135]	Effective[134]	Effective[8, 130, 132]	Effective[8]	Effective[8]	Moderate (self-evaluation)
Polishing	Very Effective[136, 144-146]	Insignificant (self-evaluation)	Effective[143]	Insignificant[143]	Very Effective[144-146]	Effective (self-evaluation)	Very Effective[144]	High (self-evaluation)
Peening	Effective[114, 136, 143]	Very Effective[142, 143]	Very Effective[143]	Very Effective[143]	Very Effective [136, 143]	Effective(self-evaluation)	Very Effective(self-evaluation)	High(self-evaluation)
Heat Treatment	Insignificant (self-evaluation)	Very Effective[137]	Insignificant[137]	Effective (self-evaluation)	Effective[138]	Insignificant (self-evaluation)	Insignificant (self-evaluation)	Moderate (self-evaluation)
Mechanical Machining	Very Effective[136, 137, 149]	Effective[136, 153]	Effective (self-evaluation)	Effective[136, 139]	Very Effective[137]	Effective (self-evaluation)	Very Effective[153]	High (self-evaluation)
Water Jet Machining	Effective [156, 157]	Effective (self-evaluation)	Effective (self-evaluation)	Effective (self-evaluation)	Effective[158, 159]	Effective (self-evaluation)	Very Effective (self-evaluation)	High (self-evaluation)
Wire EDM	Effective[165-167, 169]	Effective (self-evaluation)	Effective (self-evaluation)	Effective (self-evaluation)	Effective[165, 169]	Effective (self-evaluation)	Very Effective (self-evaluation)	High[168]

always practical for complex-shaped components [178]. Hence, several approaches are developed to determine and model the influence of "as-built metal" surface roughness on fatigue strength of SLM components under multi-axis loads. Elastic linear fracture mechanics [179] is used to determine SLM materials' fatigue behaviour. Their approach considers micro-notches as micro-cracks and indicates that the stress density factor K_1 at the crack tip is responsible for propagating cracks. Murakami [180] used linear elastic fracture mechanics method and correlated the fatigue limit with defect size. It is reported that the size and shape of the pre-existing defects in the structure affect the fatigue behaviour. However, in these approaches, determining the defect size for complex surfaces is complicated, and their applicability for multi-axis loading is minimal [178]. In approaches based on the non-local fatigue indicator parameter conducted by other researchers [181, 182], corrosion defects or fatigue behaviour can be determined from a value of the non-local fatigue indicator parameter. Other possible approaches [183, 184] aim to consider the relationships between fatigue crack initiation mechanisms, such as micro-plasticity and crack initiation from defects. However, these approaches do not allow a clear relationship between fatigue behaviour and defects. Different approaches in recent literature [185, 186] have established correlations between the non-local fatigue indicator parameter for single and multi-axis loads using extreme value statistics.

Non-local fatigue indicator parameters are used to predict the fatigue behaviour of SLM parts. These parameters take into account the microstructural features and material properties of the part beyond the immediate vicinity of the fatigue crack tip. Some of the commonly used non-local fatigue indicator parameters for SLM parts include:

1. Fatigue crack closure: This parameter considers the residual stresses and plastic deformation around the crack tip. The crack closure occurs when the crack surfaces come in contact with each other during the load cycle, leading to a reduction in the effective crack length and slowing down the crack growth rate.
2. Stress intensity factor range: This parameter is a measure of the local stress concentration at the crack tip and is related to the crack growth rate. The stress intensity factor range takes into account the cyclic loading conditions and the geometry of the part.
3. Microstructure: The microstructure of SLM parts can affect the fatigue behaviour through various mechanisms such as grain size, porosity, and surface roughness. These microstructural features can lead to stress concentration and crack initiation and can also affect the crack growth rate.
4. Residual stresses: Residual stresses in SLM parts can be introduced during the manufacturing process and can affect the fatigue behaviour by altering the stress dis-

tribution and crack growth rate. Non-local models can be used to predict the residual stress distribution and its effect on fatigue behaviour.

5. Plastic strain accumulation: This parameter considers the accumulation of plastic deformation around the crack tip during cyclic loading. The plastic strain accumulation can lead to crack initiation and growth and can also affect the crack closure behaviour.

Overall, non-local fatigue indicator parameters are important tools for predicting the fatigue behaviour of SLM parts and can be used to optimize the design and manufacturing processes to improve the fatigue performance of these parts.

4.1.1 Influence on fatigue life

According to available studies in the literature, surface morphology–induced effects on the fatigue life of SLM components are limited. However, surface-induced variations such as porosity, surface quality, residual stresses, microstructure, and other metallurgical defects profoundly affect the SLM component's fatigue life. Another typical defect other than metallurgical defects is lack of fusion, which causes irregular shape formation due to fusion interruption during the SLM process. This phenomenon is also related to fatigue life. Extensive information about how these defects occur is reported in a previously cited study [187]. Fatigue life cannot be estimated without considering surface-induced defect mechanics in modelling and manufacturing. In this context, the anisotropic properties of SLM parts based on fracture mechanics are determined and compared with the defect sensitivity of these parts using materials produced by conventional processes [188]. Maximum defect sizes are the most dominant parameter that guides the fatigue life of components. In complex shapes where lack of fusion is seen, the square root of the defect area projected in a plane normal to the stress parameter is used to determine defect size [189]. In that work, the effect of surface defects caused the low surface quality on fatigue life has been extensively described for titanium alloys and stainless steels produced with SLM. Besides, Wang et al. [190] reported that the fatigue strength of the SLM components is adversely affected if the porosity (in morphological and quantitative manners) exceeded an absolute threshold value.

In another examination, Vaysette et al. [191] reported that surface quality is one of the crucial parameters regarding the fatigue life of SLMed products. They investigated the effect of surface roughness on the high cycle fatigue life of selective laser melting and electron beam melting stress-relieved machined or as-built specimens. In addition to their tests, they utilized numerical simulations obtained with profilometer. They determined the effect of surface roughness on fatigue life using the sample surface and the associated

2D profiles. It appears that there is a significant decrease in fatigue strength for the as built samples in both production methods. On the other hand, machined samples exhibit good fatigue strength. This situation can be attributed to obtaining lower surface roughness values and relieved residual stresses after the machining process. Similar observations were obtained in different studies [178, 192–194] investigating the effect of surface quality on fatigue life of SLMed products.

Koutiri et al. [192] performed different fatigue tests to determine the number of cycles of Inconel 625 products manufactured with SLM in as-built and polished forms at different stress amplitudes. It was reported that there is an increase in the polished samples' number of cycles according to fatigue test results. It is clear that the number of cycles of the polished samples is higher than the as-built ones. They associated their result with similar defect sizes in the initial regions of both groups. More detailed information is presented in the fracture surface analysis section of their work.

Brandl et al. [153] fabricated AlSi10Mg samples with SLM in three different build orientations (0, 45, 90°) and then machined and subjected them to post-heat treatment. As a result of the investigations, they regarded the post-heat treatment process as much more effective than the build direction, considering the samples' fatigue life. They compared their results with the DIN EN 1706 standard. In addition, other defects such as porosity, residual stresses, and cracks are reduced due to lower distortion. This situation occurs since the powders' cooling rate subjected to laser beams slows after the powder bed's heat treatment. Mower and Long [195] also produced samples of AlSi10Mg with SLM, then polished the samples and compared their results with Brandl [153], stating that they exhibited lower fatigue behaviours. It should be emphasized that the difference in SLM operation and process parameters causes diverse surface-induced variations, generating the differences between these two examinations. Based on this phenomenon, it can be interpreted that the surface quality promotes different effects on fatigue life even on the same part. Therefore, it can be stated that manufacturers and researchers should consider this issue carefully. Besides, several researchers have investigated the influence of surface morphology on adhesion mechanism in the SLMed product [196]. There are different mechanisms in adhesion between two similar and dissimilar materials, such as mechanical interlocking, chemical bonding, diffusion bonding, and absorption [197]. Kinloch [198] reports that the nano- to micro-scales of surface roughness improves the influential surface area of the adhesion regime and supply a more uniform distribution of interfacial stress transfer. The high level of the balling phenomenon on the SLMed sample's surface supplies mechanical interlocking and resultant a more significant surface region for adhesion mechanism [199]. This action leads to an increment in

the general interfacial fracture toughness and accompanying strengthened adhesion behaviour in the hybrid joint. In another notable study, Zhang et al. [200] investigated the bonding mechanism and adhesion behaviour of SLMed Al_2O_3–coated stainless steels with a built horizontal and vertical surface. They reported that the bonding strength of coating in the vertically built sample shows significantly higher strength than horizontally built ones since higher surface roughness promotes a stronger adhesion mechanism between Al_2O_3 coating and stainless-steel materials.

The listed and cited works in this section mark factors effecting the fatigue life (Fig. 13) in relation to the surface morphology of the SLMed parts.

4.1.2 Influence on fatigue crack growth

Crack initiation and crack growth on SLM components' fatigue behaviour under different cyclic loads were searched in the literature for evaluation of the process-micro-/macro-structure features correlating surface-induced defects that emphasize the importance of crack related issues, but none was encountered. Even though enhancements and detailed investigations have been reported in several studies investigating the effect of manufacturing parameters on fatigue and mechanical behaviour of the SLM components, it is seen that there is an absence on the effect of surface-induced defects. It is necessary to determine to which extent crack initiation, crack growth, and fatigue cracks are affected by

surface-induced defects to obtain high fatigue performance. This decision would help us regulate the processes that have to be applied to enrich the end product surface quality, resulting in shortening the process chain and therefore cost reduction.

Riemer et al. [201] investigated the crack growth behaviour of 316L stainless steel produced with SLM under cyclic loads. They also examined the influential factors between microstructure, fatigue crack growth (FCG), and their interaction. It is reported that post-heat treated 316L exhibits high ductility behaviour, and hence, both fatigue and crack growth behaviours are not significantly affected by surface-induced defects such as porosity and internal stress. It is stated that the FCG behaviour of 316L is substantially influenced by the microstructure emerging during the solidification process. They announced that different FCG ratios are formed with the crack growth direction, depending on the grains' orientation. Due to the inadequate access in the SLM method, the opportunity to interfere with the interior surfaces is limited, making it impossible to improve the surface quality directly. In this context, Günther et al. [194] designed various diameters and numbers of inner axial channels with rough build surfaces and investigated the fatigue properties of TiAl6V4 alloys. They stated that fatigue life decreased with the increasing internal diameter, and the FCG ratio changed due to variations in ligament size. Besides, according to the fracture surface analysis, it is reported that the fatigue crack initiations mostly occurred on rough inner

Fig. 13 Factors affecting fatigue life
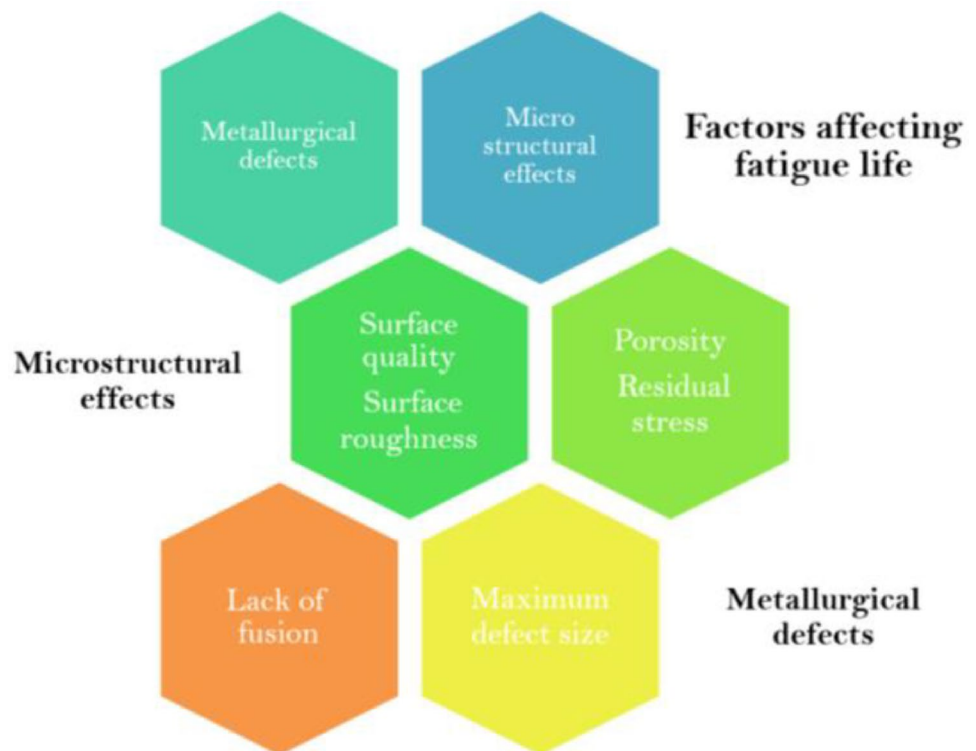
canal surfaces, and in some cases, it occurred at a point close to the machined outer surface or in an area in contact with this surface because of porosity occurring during manufacturing. One possible reason why the fatigue life decreased with increasing internal diameter for SLM products could be due to the formation of internal defects such as pores and voids. As the internal diameter of the part increases, the distance that the laser has to travel inside the part also increases. This can lead to longer exposure times, which can cause the material to overheat and potentially form defects. In addition, the internal geometry of the part can also affect the cooling rate of the molten material, which can influence the microstructure and mechanical properties of the part. The larger internal diameter can cause uneven cooling rates, which can result in residual stresses and distortion, leading to reduced fatigue life. Furthermore, the presence of residual stresses can also contribute to the reduction of fatigue life in SLM products. The internal geometry of the part can affect the distribution of residual stresses, and larger internal diameters can result in higher residual stresses, leading to a reduction in fatigue life. Overall, the relationship between internal diameter and fatigue life for SLM products is a complex one that depends on various factors, and further research is needed to fully understand and optimize the fatigue properties of SLM parts with large internal diameters. Leuders et al. [37] investigated the fatigue performance of TiAl6V4 products produced with SLM under cyclic loads with structure-defect-property relationships. They determined the behaviour of samples under HCF by fracture surface analysis. They noted that the pores very close to the

sample surface subject to relatively early failure (Fig. 14). Therefore, they are responsible for fatigue crack growth. They stated that the crack initiation could be delayed by controlling surface defects such as pores. Consequently, Leuders et al. [37] stated that micro-sized pores are the main factor influencing fatigue life and reported that residual stresses play significant roles in fatigue crack growth.

4.2 Mechanical properties of SLM components

According to the literature survey [30, 176, 202–204], it is noticed that the mechanical properties of metals and alloys produced with SLM have satisfactory features and values in comparison with other traditional production methods. It is also apparent from the data presented in Table 4 that the SLM process can impart sufficient mechanical properties compared to other conventional production methods. It is seen that a wide variety of studies have been conducted on mechanical properties within the framework of process-structure–property-performance, which are the basis of material science. In these studies, the process and surface morphology parameters categorized in Sects. 2 and 3 on the mechanical properties are characterized by their individual and combined effects. Manufacturing parameters' effects on the mechanical properties of SLM components are extensively reported in the literature. Hence, studies that include surface-induced defects such as porosity, density, structural integrity, microstructural defects, and surface quality on the mechanical properties will be mentioned briefly in this section. Nano-sized to micro-sized pores in the structure reduce

Fig. 14 The crack surfaces of SLM produced TiAl6V4 products at low magnifications (**a** and **b**); **c** and **d** high magnifications to monitor defects more precisely [37]
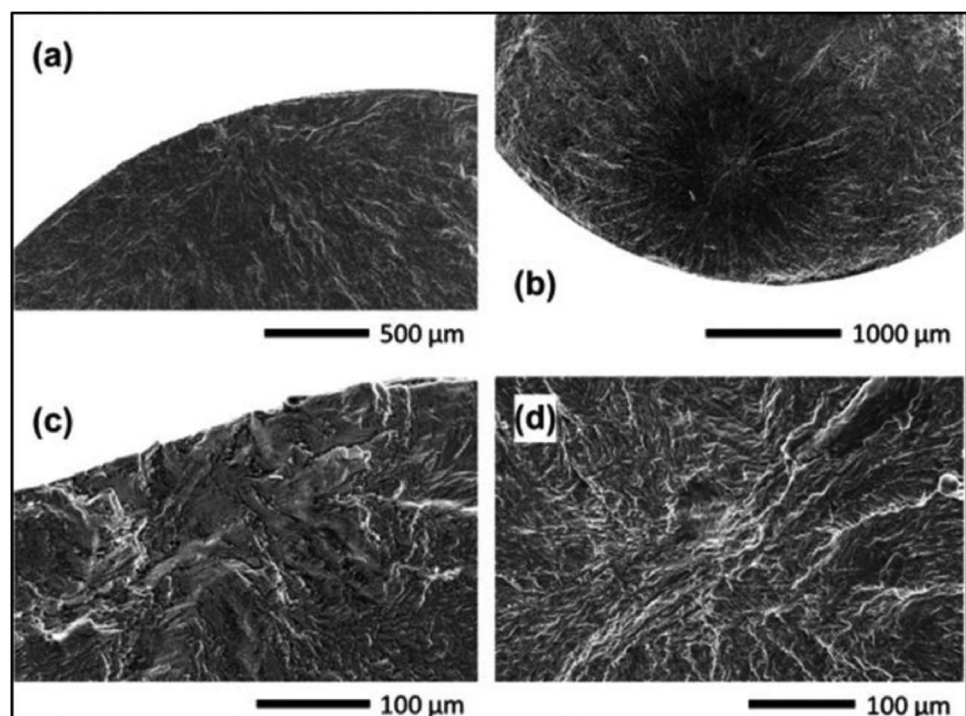
Table 4 Comparison mechanical properties of products produced by SLM and other conventional manufacturing processes

Process	Material system	Young's modulus (GPa)	Hardness (Hv)	Ultimate tensile strength (MPa)	Yield tensile strength (MPa)	Elongation at break (%)	Reference
SLM	316L	137–227	210–250 223–245	600–700 512–699	450–500 438–589	11.8–42.3	[30, 210]
SLM	AlSi10Mg	65–71	127	385–404	-	2.8–5.9	[204]
SLM	TiAl6V4	95–110 109	356–386 409	1206–951 1267	1090–1126 836–1137 1110	5.46–8.23 1.7–9.5 7.28	[73, 211, 212]
SLM	Fe–Ni	-	232	600	-	-	[213]
SLM	Fe–Ni-Cu-P	-	230	505	425	-	[214]
SLM	Pure Ti	106	248–274	757 680	555 480	19.5 17	[215, 216]
SLM	Ti2448	52–54	214–226	647–683	525–599	9.7–17.9	[216]
SLM	Inconel 718	204	-	1148 1120	907 830	25.9 25	[217, 218]
SLM	Inconel 625	-	-	940–1080	780–820	8–10	[219]
SLM	AA2618	-	-	273	191	0.6	[220]
SLM	304 SS	-	-	66–713	519–554	32.4–43.6	[221]
Annealed	Inconel 625	-	-	890	450	44	[222]
Extrusion	AA2618	-	-	392	208	13.7	[220]
Laser forming	Inconel 718	208	-	1340	1100	12	[223]
Cold work	Inconel 625	-	-	-	1100	18	[222]
Forging	316L	190–210		480–560	170–290	40	[224]
Casting	TiAl6V4	110	346	976	847	5.1	[225]
Heat-treated	Pure Ti			561	432	14.7	[226]
Casting	Inconel 718	-	-	786	488	11	[227]
Hot rolling	Ti2448	46	-	830	700	15	[228]
Hot forging	Ti alloys	55	-	755	570	13	[229]
P/M	316L	-	181–355	226–290	-	5.33–7.22	[230]
Hot extrusion	AlSi10Mg	68–72	67	178	97	15	[231]
Casting	Aluminium	71	95–133	300–365	-	3–5	[232]
Sheet forming	TiAl6V4	-	-	280	345	20	[233]

the materials' packing capacity and act as cracks by causing an increment in the stress concentration locally. This case adversely affects the mechanical properties of materials such as hardness, density, and tensile strength. Naturally, the strength of the porous material is expected to be lower than the full densified material. Also, porosity, which is inversely proportional to density, is an inevitable part of the products fabricated by SLM or other additive manufacturing (AM) methods. The number, size, shape, and location of the pores directly or indirectly affect the sintered product's mechanical properties. Indeed, porosity, density, structural integrity, and microstructural defects are factors that interact with each other and lead to significant changes in final properties. These interactions particularly make themselves visible during the consolidation of nanoparticle reinforced metal alloy powders with SLM. Nanoparticle agglomeration acts as an obstacle that slows the diffusion activity required for the

sintering process. This action deteriorates the packing ability of the powders and causes a porous structure. As a result of these porosities, microstructural defects are emerging, and structural integrity is disrupted; correspondingly, the sample's relative density and tensile strength decrease. In respect of these evaluations, Zebarjad et al. [205] reported that nanocomposite materials contain larger amounts of voids since the nanoparticles' agglomeration allows the formation of cracks and porosity. Furthermore, Dolata-Grosz et al. [206] confirmed that porosity causing low bonding between reinforcement and matrix material is a significant indicator of the degradation of mechanical properties. Moreover, various researchers [75, 207–209] have reported an increase in mechanical properties associated with improved surface quality resulting from increased hardness and lower delamination, which is suppressed by residual compressive stress on the material surface.

4.2.1 Influence on density

High final density is achieved by reducing porosities and ensuring better structural integrity. There is a close correlation between SLM process parameters and the density of materials. Products with a density of 99.9% can be achieved thanks to a good agreement between process parameters and surface variables. The laser ED, expressing the energy per unit volume for a powder particle by the laser beam, is a key factor that plays an essential role in SLM products' quality and performance [26]. The ED varies depending on laser power (p), scanning speed (v), hatching distance (h), and layer thickness (s) are given in Eq. 1. Generally, the incoming energy density is expected to be high to achieve a maximum amount of melting. This occasion leads to an increase in the final density of the product. In other words, the energy density can be improved by providing the desired control (increase or decrease) of the variables given in Eq. 1 to produce products with the highest possible density. However, ED is not sufficient to achieve the density goal alone. Other process and post-process parameters such as scanning speed, surface orientation, scanning pattern, cooling rate, heat transfer, and interface compatibility are necessary to be optimized, directly or indirectly affecting the product's density and final properties.

$$ED = \frac{p}{v \cdot h \cdot s} \tag{1}$$

Figure 15 illustrates the relative density of as-built AlSi10Mg samples with fabricated SLM process as a function of diverse energy densities [234]. Authors stated that the samples produced in the energy density range of 145–175 J/

mm^3 exhibit higher relative densities (98.17%) comparing to other energy density levels. They also observed that samples with lower relative density exist in these high-energy ranges. They attributed this to the powder bed pool, which does not completely melt due to various process parameters, oxides, porosities, and other metallurgically induced defects.

4.2.2 Influence on tensile properties

Tensile properties essentially vary depending on the relative densities of the product [235]. However, powder properties such as powder morphology, size, and distribution, the crystallographic structure of powders together with various process parameters, such as scanning speed, scanning pattern, and laser power, are also highly effective on the relative density [221]. Moreover, the powders' packing characteristics and consolidation behaviour are factors that profoundly influence the relative density of the sample and resultant tensile properties. For instance, the effect of different particle size distributions on tensile properties is investigated in [96]. Their outcomes revealed that the SLMed products with smaller particle sizes show higher tensile strength than coarse particle sizes. It is reported that the difference in tensile properties refers to coarse particle sizes contain more pores than small particles. They attributed this to vacancies, which are occurred during the production process in bigger particles. They also stated that particle size distribution has a substantial effect not only on the tensile properties of the products but also on the surface quality and density. It is announced that processing parameters, especially the building direction, also significantly affect the tensile properties as well as the powder characteristics.

Fig. 15 The relative density of AlSi10Mg samples with fabricated SLM process as a function of different energy densities [234]
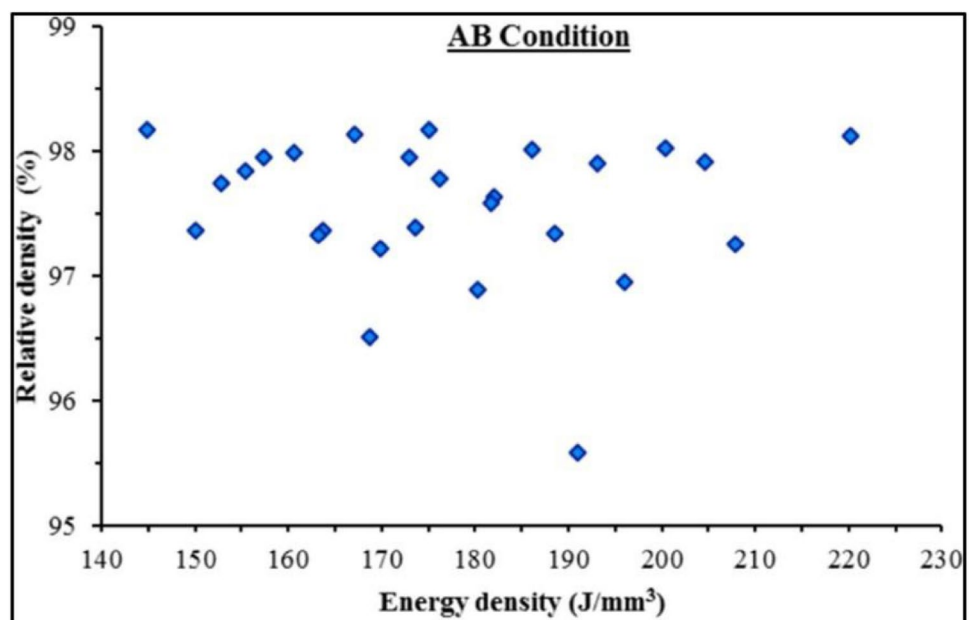
To determine how the micro-voids behaved during the tensile test, Simonelli et al. [85] tested TiAl6V4 samples up to the necking region and then stopped the test. They then examined the microstructure analysis of the tensile specimens exposed to plastic deformation. They stated that it could not be determined clearly whether the formed micro-cavity is due to the pre-existing pores resulting from the manufacturing process or alpha lath fracture in the structure. However, they reported that the micro-voids trigger crack initiation and tend to spread along α grain boundary. This indicates that surface-induced defects such as micro-voids in this case adversely affect the structural integrity and final properties of the products. Based on the above discourse, it can be inferred that the evaluations and comments made in this study are very well in agreement with the available studies in the literature [85, 203, 221]. Accordingly, this section can be summarized by Fig. 16, in the light of the discussed phenomena by the information and assertations in the cited literature works.

4.2.3 Influence on microhardness

Microhardness mainly depends on the product's microstructure and the porosity (size and distribution), which are surface-induced variations in the structure. On the other hand, surface-induced variations are significantly affected by process parameters, as mentioned earlier. In this context, various studies in the literature examine changes in microhardness depending on manufacturing strategies such as laser parameters [236], energy densities [237], laser power [238], and cutting planes [239]. Besides, the studies which are dealing with the effect of reinforcement materials [236, 240] (type, ratio) and alloying elements [241] on microhardness exist. It is reported that microhardness increases with the increment of hard ceramic particles [242]. Although this is the correct approach, in some cases, the morphology and distribution of the reinforcement materials influence the microstructural development and naturally microhardness. For example, Gu et al. [243] reached the maximum microhardness value in 12.5 wt% TiC reinforced Ti matrix composites. After this value, they found that microhardness tends to decline with

Fig. 16 Influencing factor on tensile properties of SLMed parts
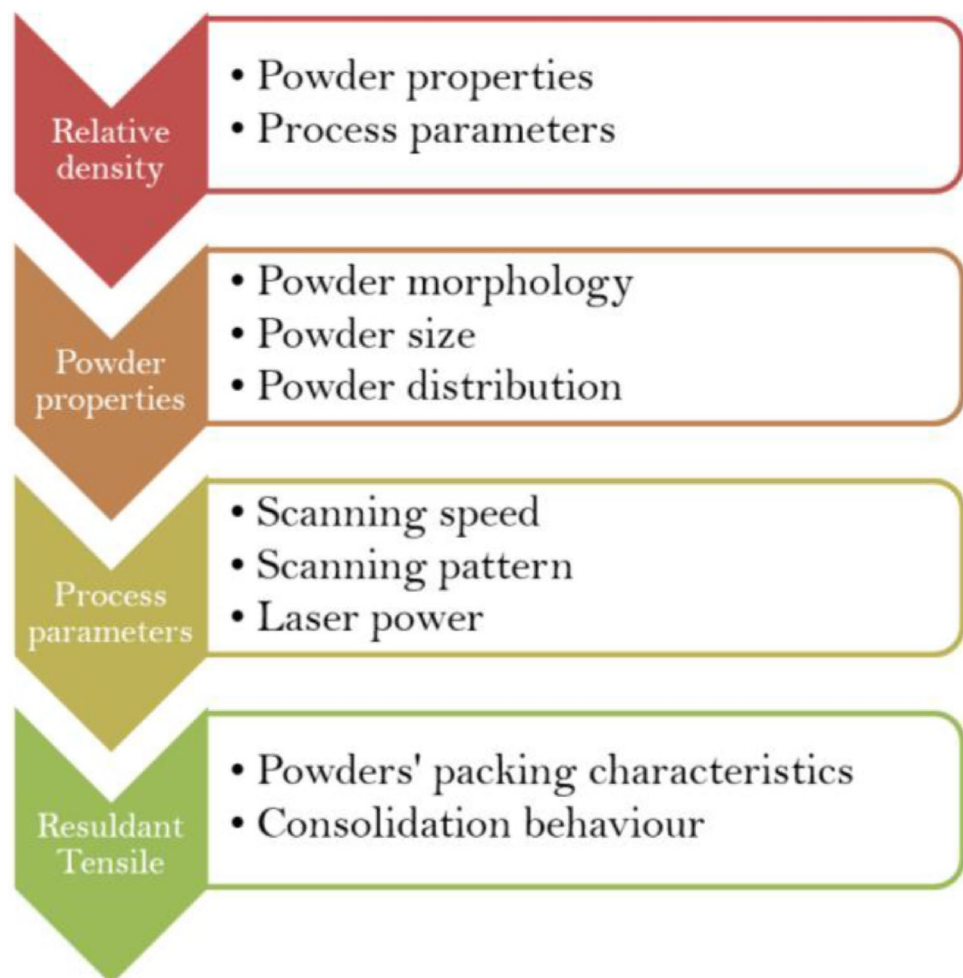
increasing reinforcement ratio, as shown in Fig. 17. They stated that the morphology and distribution of TiC in their system are responsive to the volume fraction, and beyond the critical threshold value, it adversely affects the nanostructure and causes the formation of a porous structure. It can be deduced from these outcomes that the different parameters in the SLM process, reinforcement material (ratio, morphology, type), and the chemical composition of the material cause substantial alterations in the microstructural characteristics and consequently the microhardness.

To overcome the rough surface of SLMed metallic alloys, various surface modification techniques such as ultrasonic nanocrystal surface modification [208], multi-pass ultrasonic surface rolling [244], and surface mechanical attrition [245] are regarded as beneficial post-treatment approaches. The main target of applying these surface modification techniques is to improve the surface hardness by generating severe plastic deformation on the product's surface. For instance, Zhao et al. [246] proposed enhancing the hardness and wear resistance of commercial pure titanium (CP-Ti)/TiN alloys by using gas nitriding. For this purpose, they prepared CP-Ti samples with different gas nitriding under high purity Ar and N_2 atmosphere. As shown in Fig. 18a, nitride-coated samples exhibited significantly higher hardness than un-coated and Ar-coated samples. Plus, they employed surface profiles and scanning electron microscope (SEM) analyses to evaluate wear scars of samples, as shown in Fig. 18b. They stated that the N0 sample shows a shallow and narrow wear scar compared to S0 and A0 samples due to increased surface hardness resulting from N_2 nitriding.

5 Modeling and simulation of surface morphology in SLM

Mathematical modeling and computer simulations are essential tools in engineering, allowing engineers to simulate complex systems and predict their behaviour under different conditions. These tools can be used to optimize designs, reduce costs, and minimize risks associated with real-world testing. In engineering, mathematical models are used to describe the physical behaviour of a system in terms of mathematical equations, while computer simulations use these models to predict the behaviour of the system in response to different inputs. This allows engineers to test and refine their designs before building physical prototypes, saving time and resources. The importance of engineering mathematical modeling and computer simulations cannot be overstated, as they allow engineers to simulate and analyse systems that are too complex, expensive, or dangerous to test in the real world. This not only helps to ensure the safety and reliability of engineering designs but also drives innovation and the development of new technologies. Therefore, in this part, we would like to mention the most prominent and recent modelling and simulation studies in the literature towards SLM-surface morphology correlation.

Fig. 17 Microhardness values of SLM-produced Ti/TiC samples with different reinforcement ratios and matching indentation surfaces [243]
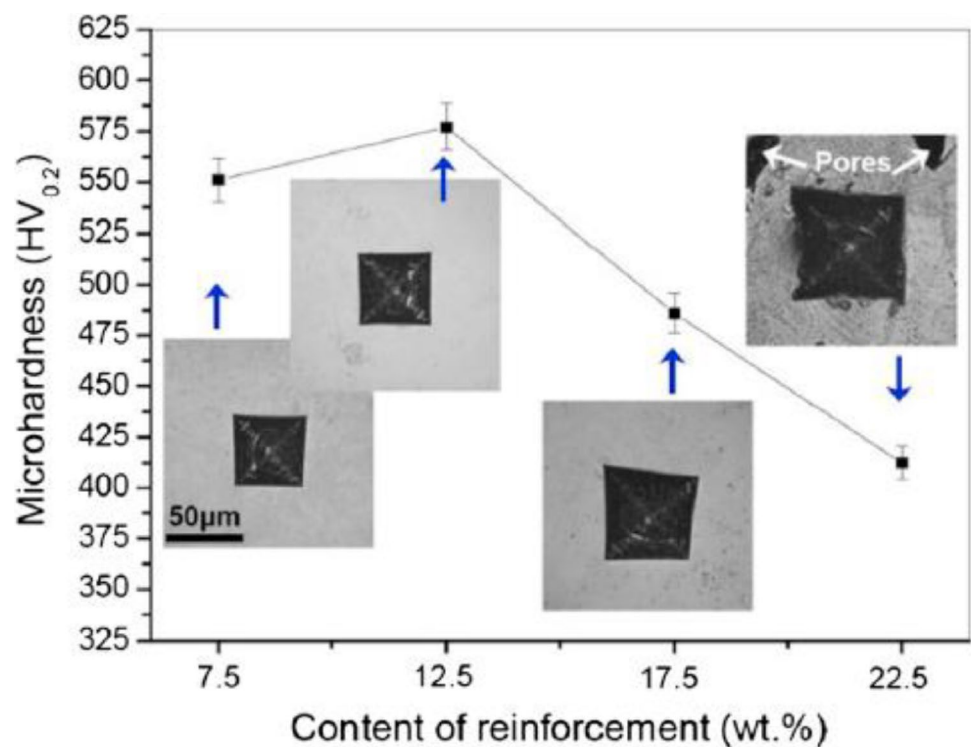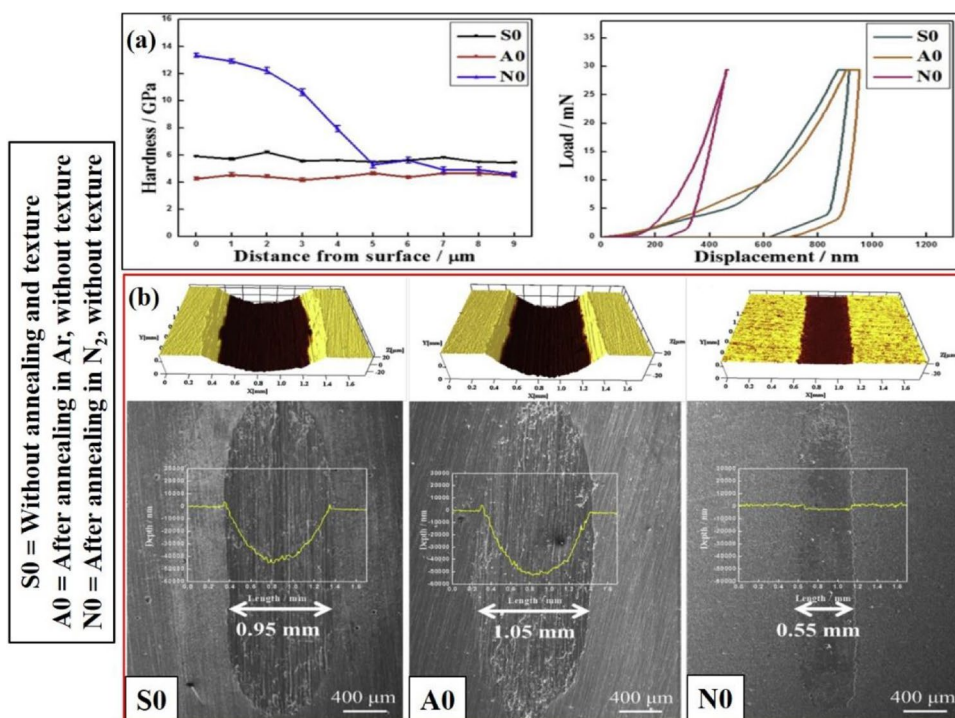
Fig. 18 (**a**) Hardness variations from the exterior surface of different post-treated samples and (**b**) their surface profile and morphology [246]

S0 = Without annealing and texture
A0 = After annealing in Ar, without texture
N0 = After annealing in N₂, without texture

Finite element method has been employed by Cutolo et al. [247] for simulations of laser powder bed fusion of Ti6Al4V. The authors lay out surface conditions by the simulation. Several surface finishing steps are considered. The ex situ TiN reinforced IN718 with high fidelity numerical simulations has been reported by Mandal et al. [248]. A phase field 2D numerical model is described in the work. Jiabao et al. [249] tracked surface morphology evolution of a stainless steel by a multi scale numerical model. They report good agreement between numerical and experimental data. The authors provide a simulation sourced animation of transient temperature distribution of the SLM process. Particularly, the paper of Jiabao et al. [249] is a prominent example of simulations toward surface morphology evaluation of SLMed parts. Another great numerical simulation has been reported by Li et al. [250]. The authors focus on laser polishing of SLMed 316L steel in terms of surface quality. They evaluated surface morphology by qualitative and quantitative measures while providing spatial visuals by the simulation results. To simulate the flow of molten metal, the evolution of surface morphology, and the formation of defects during the cooling stage, multi-physics models were created and explained by the authors. Wang et al. [251] have used crystal plasticity finite element method in order to simulate SLMed 316L stainless steel. Again, predictions based on the simulation results are stated to be in well orientation with the experimental results. Spatial resolution alongside with regional grouping and mod identification tasks are realized by the authors. Pilgar et al. [252] have benefitted a numerical

model in order to predict fatigue of SLMed Hastelloy-X. The paper mostly mention surface in terms of relationship between surface roughness and the fatigue behaviour. Particle hydrodynamics for numerical simulations towards SLM process has been studied by Long and Huang [253], focusing on particle smoothing. The paper reports numerical method improvements in smoothed particle hydrodynamics, kernel gradient correction, and surface tension model. The paper is a prominent one in terms of model descriptions and modifications. Initial state of a square shaped droplet is given and then the smoothed particle transitions are expressed with three different visuals. However, surface morphology aspects of the SLMed part are absent in the work. Peng et al. [254] have used molecular dynamics simulations in order to study surface integrity of additive manufacturing parts for multi-principal element alloys (FeCrNi). They have also benefited from artificial neural network machine learning method for supporting their model. They build a correlation between laser power and scan speed with the surface. They state that scan speed has a bigger effect than laser speed in terms of surface roughness and quality. Atomic simulation results pose very detailed spatial resolution.

6 Conclusions

Surface morphology properties in accordance with SLM production have been reviewed in the presented work. Surface morphology variants induced by process

parameters are categorized comprehensively in the sub-headings. Furthermore, surface morphology enhancement and the effects of surface-induced variations on SLM-produced metal alloys' behaviour are explained. Surface variations resulting from process and post-treatment parameters based on the intended application and the effect of these variations on SLMed product behaviour are summarized. Knowledge of these variables provides a basic understanding of overcoming the challenges of producing metal alloys for various industrial and technological applications associated with the SLM process. Following evaluations and deductions can be obtained according to conducted survey:

1. It is seen that process parameters are systematically studied, and better surface quality and favourable surface morphology of as build surfaces are possible. However, various industrial applications necessitate further enhancement and improvement of surface qualifications.
2. In situ and post-processing provide necessary qualification of surface quality and morphology according to specific needs of industrial applications, but the main concern is on increased total cost for those techniques.
3. Ti6Al4V alloy is the most encountered SLMed alloy in the literature, most probably due to its medical usage.
4. Components with a relatively defect-free structure can be attained with the SLM process by filling the pores between metal powders and increasing the surface quality by controlling the parameters that have important influences on surface-induced variables such as residual stress, porosity, structural integrity, and microstructure.
5. By additional measures such as in situ surface improvement, post-processing, and finishing, surface properties can be substantially improved.
6. In situ treatment such as base plate heating and re-scanning mostly focus on relieving residual stresses and releasing trapped gasses.
7. Base plate heating and powder preheating may decrease the necessity of re-scanning, leading to more production efficiency and lower operational costs since re-scanning is a very time demanding task and should be controlled very carefully.
8. Re-scanning, a technique in order to improve surface quality, may have adverse effects if laser processing parameters are not selected carefully. Re-scanning provides feasibility for the post-machining of the surfaces.
9. Heat treatment as a post-processing technique for the SLMed part seems to have a minimal effect on surface roughness and morphology. Peening and polishing have higher effects on the surface comparing to heat treatment.
10. Machinability and its surface impacts are studied mainly for mechanical machining such as grinding and milling. EDM and water jet studies are very limited in terms of surface morphology.
11. The correlation between surface morphology of SLMed parts and mechanical properties is relatively weak comparing to SLM production parameters.
12. Some mechanical properties reported for metallic systems produced with the SLM approach exceed similar materials obtained by conventional manufacturing methods. However, few published studies examine the effect of surface-induced variations on behaviours such as low cycle fatigue, fatigue crack growth, fracture toughness, tensile strength, impact, creep, and creep-fatigue.

7 Challenges and future work

Based on the present literature survey, following challenges are identified and accordingly some future study recommendations are asserted.

1. Limited examinations about the effect of powder particle sizes, particle size distributions, and particularly the rheological properties of powders on the surface quality were encountered. Detailed characterization of these parameters' effects should be addressed in future works.
2. Multiple parameter correlations of SLM process parameters should be identified by experimental works.
3. Since shrinkage, residual stresses, and fatigue behaviour effect surface morphology of final product, especially for fully dense category, more literature report is anticipated in relation with surface properties.
4. Re-scanning can be much more effective with in situ monitoring, image processing, and machine decision-making. Tracks to be skipped in terms of re-scan should be identified after the first scan. This arises the need of control theory and in the light of recent developments in artificial intelligence, image processing, precision measurement, fast response measurement equipment, and very capable computing.
5. Digital twin concept by machine learning methods should be considered for generalization of scientific results.
6. Post-treatment and post-processing of SLMed parts to obtain favourable surface roughness and quality have uncertain and indefinite terminology that cannot separate them from one another. Using "non-material removal" type terms may not be a reasonable classification. Better terminological integrity is needed for a common literature.

7. Surface morphology should be studied after water jet and EDM cutting of SLMed parts as future research topics.

8. A comprehensive and common database is necessary for training machine learning approaches that can aid adaptive neuro-fuzzy inference system (ANFIS) type decision-making algorithms for in situ treatment approaches. By this way, SLM can give better surface quality with less human experience and interference.

9. Finally, as an emerging technology for vast production of industrial items, systematic studies seem to be necessary for mathematical modelling and reduction of experimental results. Statistical evaluations of parameter combinations, statistical and machine learning methods for data interpolation, and benchmarking of optimization algorithms are prone to future research.

Declarations

Ethics approval and consent to participate Not applicable.

Consent for publication The consent to submit this paper has been received explicitly from all co-authors.

Competing interests The authors declare no competing interests.

References

1. Waqar S, Liu J, Sun Q, Guo K, Sun J (2020) Effect of post-heat treatment cooling on microstructure and mechanical properties of selective laser melting manufactured austenitic 316L stainless steel. Rapid Prototyp J 26(10):1739–1749
2. Dong D et al (2021) Selective laser melting (SLM) of CX stainless steel: theoretical calculation, process optimization and strengthening mechanism. J Mater Sci Technol 73:151–164
3. Chen P et al (2020) Fabricating CoCrFeMnNi high entropy alloy via selective laser melting in-situ alloying. J Mater Sci Technol 43:40–43
4. Yu W et al (2019) Influence of re-melting on surface roughness and porosity of AlSi10Mg parts fabricated by selective laser melting. J Alloy Compd 792:574–581
5. Salman O et al (2019) Impact of the scanning strategy on the mechanical behavior of 316L steel synthesized by selective laser melting. J Manuf Process 45:255–261
6. Yu WH et al (2019) Particle-reinforced metal matrix nanocomposites fabricated by selective laser melting: a state of the art review. Prog Mater Sci 104:330–379
7. Gorji N, O'Connor R, Brabazon D (2019) XPS, XRD, and SEM characterization of the virgin and recycled metallic powders for 3D printing applications. In IOP Conference Series. Mater Sci Eng 591(1):012016. IOP Publishing.
8. Pal S, Lojen G, Hudak R, Rajtukova V, Brajlih T, Kokol V, Drstvenšek I (2020) As-fabricated surface morphologies of Ti-6Al-4V samples fabricated by different laser processing parameters in selective laser melting. Addit Manuf 33:101147
9. Binali R et al (2023) Machinability investigations based on tool wear, surface roughness, cutting temperature, chip morphology and material removal rate during dry and MQL-assisted milling of Nimax mold steel. Lubricants 11(3):101
10. Binali R, Yaldız S, Neşeli S (2021) S960QL Yapı Çeliğinin İşlenebilirliğinin Sonlu Elemanlar Yöntemi ile İncelenmesi. Avrupa Bilim ve Teknoloji Dergisi 31:85–91
11. Demir H, Ulas H, Binali R (2018) Investigation of the effects on surface roughness and tool wear in the toolox44 material. Technol Appl Sci 13:19–28
12. Mikolajczyk T et al (2022) Research on using an unconventional tool for increasing tool life by selective exchange of worn cutting edge. Appl Sci 13(1):460
13. Yan Q, Song B, Shi Y (2020) Comparative study of performance comparison of AlSi10Mg alloy prepared by selective laser melting and casting. J Mater Sci Technol 41:199–208
14. Xiong Z et al (2019) Selective laser melting of NiTi alloy with superior tensile property and shape memory effect. J Mater Sci Technol 35(10):2238–2242
15. Chastand V et al (2018) Comparative study of fatigue properties of Ti-6Al-4V specimens built by electron beam melting (EBM) and selective laser melting (SLM). Mater Charact 143:76–81
16. Binali R, Yaldız S, Neşeli S (2022) Investigation of power consumption in the machining of S960QL steel by finite elements method. Eur J Tech (EJT) 12(1):43–48
17. Ning J et al (2019) Analytical modeling of 3D temperature distribution in selective laser melting of Ti-6Al-4V considering part boundary conditions. J Manuf Process 44:319–326
18. Aboulkhair NT et al (2014) Reducing porosity in AlSi10Mg parts processed by selective laser melting. Addit Manuf 1:77–86
19. Zhou X et al (2015) 3D-imaging of selective laser melting defects in a Co–Cr–Mo alloy by synchrotron radiation micro-CT. Acta Mater 98:1–16
20. Zhang S et al (2013) Cracking behavior and formation mechanism of TC4 alloy formed by selective laser melting. J Mech Eng 49(23):21–27
21. Anwar AB, Pham Q-C (2018) Study of the spatter distribution on the powder bed during selective laser melting. Addit Manuf 22:86–97
22. Sun Y et al (2020) High-temperature oxidation behavior and mechanism of Inconel 625 super-alloy fabricated by selective laser melting. Opt Laser Technol 132:106509

23. Li R et al (2010) Densification behavior of gas and water atomized 316L stainless steel powder during selective laser melting. Appl Surf Sci 256(13):4350–4356

24. Kang N et al (2017) Microstructure and strength analysis of eutectic Al-Si alloy in-situ manufactured using selective laser melting from elemental powder mixture. J Alloy Compd 691:316–322

25. Liu S, Shin YC (2019) Additive manufacturing of Ti6Al4V alloy: a review. Mater Des 164:107552

26. Tonelli L, Fortunato A, Ceschini L (2020) CoCr alloy processed by selective laser melting (SLM): effect of laser energy density on microstructure, surface morphology, and hardness. J Manuf Process 52:106–119

27. Lin K, Yuan L, Gu D (2019) Influence of laser parameters and complex structural features on the bio-inspired complex thin-wall structures fabricated by selective laser melting. J Mater Process Technol 267:34–43

28. Sun D et al (2019) Selective laser melting of titanium parts: influence of laser process parameters on macro-and microstructures and tensile property. Powder Technol 342:371–379

29. Yang T et al (2019) The influence of process parameters on vertical surface roughness of the AlSi10Mg parts fabricated by selective laser melting. J Mater Process Technol 266:26–36

30. Liverani E et al (2017) Effect of selective laser melting (SLM) process parameters on microstructure and mechanical properties of 316L austenitic stainless steel. J Mater Process Technol 249:255–263

31. Shi X et al (2017) Parameter optimization for Ti-47Al-2Cr-2Nb in selective laser melting based on geometric characteristics of single scan tracks. Opt Laser Technol 90:71–79

32. Catchpole-Smith S et al (2017) Fractal scan strategies for selective laser melting of 'unweldable' nickel superalloys. Addit Manuf 15:113–122

33. Wang D et al (2017) Mechanisms and characteristics of spatter generation in SLM processing and its effect on the properties. Mater Des 117:121–130

34. Mei X et al (2019) Interfacial characterization and mechanical properties of 316L stainless steel/Inconel 718 manufactured by selective laser melting. Mater Sci Eng: A 758:185–191

35. Shi Q et al (2016) Effects of laser processing parameters on thermal behavior and melting/solidification mechanism during selective laser melting of TiC/Inconel 718 composites. Opt Laser Technol 84:9–22

36. Cherry J et al (2015) Investigation into the effect of process parameters on microstructural and physical properties of 316L stainless steel parts by selective laser melting. Int J Adv Manuf Technol 76(5–8):869–879

37. Leuders S et al (2013) On the mechanical behaviour of titanium alloy TiAl6V4 manufactured by selective laser melting: fatigue resistance and crack growth performance. Int J Fatigue 48:300–307

38. Schleifenbaum H et al (2010) Individualized production by means of high power selective laser melting. CIRP J Manuf Sci Technol 2(3):161–169

39. Malkorra I et al (2020) The influence of the process parameters of drag finishing on the surface topography of aluminium samples. CIRP J Manuf Sci Technol 31:200–209

40. Zhang J, Chaudhari A, Wang H (2019) Surface quality and material removal in magnetic abrasive finishing of selective laser melted 316L stainless steel. J Manuf Process 45:710–719

41. Cabanettes F et al (2018) Topography of as built surfaces generated in metal additive manufacturing: a multi scale analysis from form to roughness. Precis Eng 52:249–265

42. Lou S et al (2019) Characterisation methods for powder bed fusion processed surface topography. Precis Eng 57:1–15

43. Lesyk D et al (2020) Post-processing of the Inconel 718 alloy parts fabricated by selective laser melting: effects of mechanical surface treatments on surface topography, porosity, hardness and residual stress. Surf Coat Technol 381:125136

44. Thompson A et al (2017) Topography of selectively laser melted surfaces: a comparison of different measurement methods. CIRP Ann 66(1):543–546

45. Artigas R (2011) Imaging confocal microscopy. Optical measurement of surface topography. Springer, pp 237–286

46. de Groot P (2011) Coherence scanning interferometry. Optical measurement of surface topography. Springer, pp 187–208

47. Dursun G, Ibekwe S, Li G, Mensah P, Joshi G, Jerro D (2020) Influence of laser processing parameters on the surface characteristics of 316L stainless steel manufactured by selective laser melting. Mater Today Proc 26:387–393

48. Liu Y et al (2018) Investigation into the influence of laser energy input on selective laser melted thin-walled parts by response surface method. Opt Lasers Eng 103:34–45

49. Sing SL, Wiria FE, Yeong WY (2018) Selective laser melting of titanium alloy with 50 wt% tantalum: effect of laser process parameters on part quality. Int J Refract Metal Hard Mater 77:120–127

50. Hu X et al (2019) Laser welding of a selective laser melted Ni-base superalloy: microstructure and high temperature mechanical property. Mater Sci Eng: A 745:335–345

51. Chen Z et al (2018) Surface roughness of selective laser melted Ti-6Al-4V alloy components. Addit Manuf 21:91–103

52. Mumtaz KA, Hopkinson N (2009) Top surface and side roughness of Inconel 625 parts processed using selective laser melting. Rapid Prototyp J 15(2):96–103

53. Chen Z et al (2017) Experimental research on selective laser melting AlSi10Mg alloys: process, densification and performance. J Mater Eng Perform 26(12):5897–5905

54. Darvish K et al (2018) Selective laser melting of Co-29Cr-6Mo alloy with laser power 180–360 W: cellular growth, intercellular spacing and the related thermal condition. Mater Charact 135:183–191

55. Rao H et al (2016) The influence of processing parameters on aluminium alloy A357 manufactured by Selective Laser Melting. Mater Des 109:334–346

56. Zhao C et al (2017) Real-time monitoring of laser powder bed fusion process using high-speed X-ray imaging and diffraction. Sci Rep 7(1):1–11

57. Gu D et al (2012) Densification behavior, microstructure evolution, and wear performance of selective laser melting processed commercially pure titanium. Acta Mater 60(9):3849–3860

58. Dong Z et al (2019) Effect of hatch spacing on melt pool and as-built quality during selective laser melting of stainless steel: modeling and experimental approaches. Materials 12(1):50

59. Huang Y et al (2016) Finite element analysis of thermal behavior of metal powder during selective laser melting. Int J Therm Sci 104:146–157

60. Hu Z et al (2017) Experimental investigation on selective laser melting of 17–4PH stainless steel. Opt Laser Technol 87:17–25

61. Thijs L et al (2010) A study of the microstructural evolution during selective laser melting of Ti–6Al–4V. Acta Mater 58(9):3303–3312

62. Parry L, Ashcroft I, Wildman RD (2016) Understanding the effect of laser scan strategy on residual stress in selective laser melting through thermo-mechanical simulation. Addit Manuf 12:1–15

63. Wan H et al (2018) Effect of scanning strategy on grain structure and crystallographic texture of Inconel 718 processed by selective laser melting. J Mater Sci Technol 34(10):1799–1804

64. Cheng B, Shrestha S, Chou K (2016) Stress and deformation evaluations of scanning strategy effect in selective laser melting. Addit Manuf 12:240–251

65. Song J et al (2018) Role of scanning strategy on residual stress distribution in Ti-6Al-4V alloy prepared by selective laser melting. Optik 170:342–352

66. Mugwagwa L et al (2019) Evaluation of the impact of scanning strategies on residual stresses in selective laser melting. Int J Adv Manuf Technol 102(5–8):2441–2450

67. Koutny D et al (2018) Influence of scanning strategies on processing of aluminum alloy EN AW 2618 using selective laser melting. Materials 11(2):298

68. Ukwattage AK, Achuthan A (2018) Development of residual stress of parts fabricated via Selective Laser Melting (SLM) techniques under di erent scanning strategies. In 2018 AIAA/ASCE/AHS/ASC Structures. Struct Dyn Mater Conf 0090

69. AlMangour B, Grzesiak D, Yang J-M (2017) Scanning strategies for texture and anisotropy tailoring during selective laser melting of TiC/316L stainless steel nanocomposites. J Alloy Compd 728:424–435

70. Kemerling B et al (2018) Residual stress evaluation of components produced via direct metal laser sintering. Weld World 62(3):663–674

71. Kruth J-P et al (2012) Assessing and comparing influencing factors of residual stresses in selective laser melting using a novel analysis method. Proc Inst Mech Eng Part B: J Eng Manuf 226(6):980–991

72. Zaeh MF, Branner G (2010) Investigations on residual stresses and deformations in selective laser melting. Prod Eng Res Devel 4(1):35–45

73. Ali H, Ghadbeigi H, Mumtaz K (2018) Effect of scanning strategies on residual stress and mechanical properties of selective laser melted Ti6Al4V. Mater Sci Eng: A 712:175–187

74. Wang L-Z, Wang S, Wu J-J (2017) Experimental investigation on densification behavior and surface roughness of AlSi10Mg powders produced by selective laser melting. Opt Laser Technol 96:88–96

75. Gupta MK et al (2020) Impact of layer rotation on micro-structure, grain size, surface integrity and mechanical behaviour of SLM Al-Si-10Mg alloy. J Market Res 9(5):9506–9522

76. Geiger F, Kunze K, Etter T (2016) Tailoring the texture of IN738LC processed by selective laser melting (SLM) by specific scanning strategies. Mater Sci Eng: A 661:240–246

77. Strano G et al (2013) Surface roughness analysis, modelling and prediction in selective laser melting. J Mater Process Technol 213(4):589–597

78. Li Z et al (2018) The influence of scan length on fabricating thin-walled components in selective laser melting. Int J Mach Tools Manuf 126:1–12

79. Parry L, Ashcroft I, Wildman R (2019) Geometrical effects on residual stress in selective laser melting. Addit Manuf 25:166–175

80. Yadroitsev I, Smurov I (2011) Surface morphology in selective laser melting of metal powders. Phys Procedia 12:264–270

81. Savalani MM, Pizarro JM (2016) Effect of preheat and layer thickness on Selective Laser Melting (SLM) of magnesium. Rapid Prototyp J 22(1):115–122

82. Weißmann V et al (2018) Effects of build orientation on surface morphology and bone cell activity of additively manufactured Ti6Al4V specimens. Materials 11(6):915

83. Tuomi JT et al (2017) In vitro cytotoxicity and surface topography evaluation of additive manufacturing titanium implant materials. J Mater Sci - Mater Med 28(3):53

84. Mumtaz K, Hopkinson N (2010) Selective laser melting of Inconel 625 using pulse shaping. Rapid Prototyp J 16(4):248–257

85. Simonelli M, Tse YY, Tuck C (2014) Effect of the build orientation on the mechanical properties and fracture modes of SLM Ti–6Al–4V. Mater Sci Eng: A 616:1–11

86. Metelkova J et al (2018) On the influence of laser defocusing in selective laser melting of 316L. Addit Manuf 23:161–169

87. Pal S et al (2018) Evolution of metallurgical properties of Ti-6Al-4V alloy fabricated in different energy densities in the selective laser melting technique. J Manuf Process 35:538–546

88. Zuo P et al (2019) Microstructure evolution of 24CrNiMoY alloy steel parts by high power selective laser melting. J Manuf Process 44:28–37

89. Carluccio D et al (2019) The influence of laser processing parameters on the densification and surface morphology of pure Fe and Fe-35Mn scaffolds produced by selective laser melting. J Manuf Process 40:113–121

90. Razavykia A et al (2020) An overview of additive manufacturing technologies—a review to technical synthesis in numerical study of selective laser melting. Materials 13(17):3895

91. Zhang J et al (2019) A review of selective laser melting of aluminum alloys: processing, microstructure, property and developing trends. J Mater Sci Technol 35(2):270–284

92. Mercelis P, Kruth JP (2006) Residual stresses in selective laser sintering and selective laser melting. Rapid Prototyp J 12(5):254–265

93. Chen C et al (2019) Effect of overlap rate and pattern on residual stress in selective laser melting. Int J Mach Tools Manuf 145:103433

94. Kruth JP, Badrossamay M, Yasa E, Deckers J, Thijs L, Van Humbeeck J (2010) Part and material properties in selective laser melting of metals. In Proceedings of the 16th International Symposium on Electromachining (ISEM XVI). Shanghai Jiao Tong Univ Press, pp 3–14

95. Yang E et al (2019) Effect of geometry on the mechanical properties of Ti-6Al-4V Gyroid structures fabricated via SLM: a numerical study. Mater Des 184:108165

96. Spierings AB, Herres N, Levy G (2011) Influence of the particle size distribution on surface quality and mechanical properties in AM steel parts. Rapid Prototyp J 17(3):195–202

97. Zhou Y, Ning F (2020) Build orientation effect on geometric performance of curved-surface 316L stainless steel parts fabricated by selective laser melting. ASME J Manuf Sci Eng 142(12):121002. https://doi.org/10.1115/1.4047624

98. Lee YS, Zhang W (2015) Mesoscopic simulation of heat transfer and fluid flow in laser powder bed additive manufacturing. In 2015 International Solid Freeform Fabrication Symposium. University of Texas at Austin

99. Savalani MM, Hao L, Dickens PM, Zhang Y, Tanner KE, Harris RA (2012) The effects and interactions of fabrication parameters on the properties of selective laser sintered hydroxyapatite polyamide composite biomaterials. Rapid Prototyp J 18(1):16–27

100. Dingal S et al (2008) The application of Taguchi's method in the experimental investigation of the laser sintering process. Int J Adv Manuf Technol 38(9–10):904–914

101. Hon KKB (2007) Digital additive manufacturing: from rapid prototyping to rapid manufacturing. In Proceedings of the 35th International MATADOR Conference: Formerly The International Machine Tool Design and Research Conference. Springer, London, pp 337–340

102. Nguyen Q et al (2018) The role of powder layer thickness on the quality of SLM printed parts. Arch Civil Mech Eng 18:948–955

103. Triantaphyllou A et al (2015) Surface texture measurement for additive manufacturing. Surf Topogr Metrol Prop 3(2):024002

104. Jiang J, Xu X, Stringer J (2018) Support structures for additive manufacturing: a review. J Manuf Mater Process 2(4):64

105. Günaydın AC, Yıldız AR, Kaya N (2022) Multi-objective optimization of build orientation considering support structure volume and build time in laser powder bed fusion. Mater Test 64(3):323–338

106. Aslan B, Yıldız AR (2020) Optimum design of automobile components using lattice structures for additive manufacturing. Mater Test 62(6):633–639

107. Mugwagwa L, Dimitrov D, Matope S, Muvunzi R (2016) Residual stresses and distortions in selective laser meltinga review. In Proceedings of the 17th Rapid Product Development Association of South Africa, Vanderbijlpark, South Africa, pp 2–4

108. Martin AA (2019) Ultrafast dynamics of laser-metal interactions in additive manufacturing alloys captured by in situ X-ray imaging. Mater Today Adv 1:100002

109. Boschetto A, Bottini L, Veniali F (2017) Roughness modeling of AlSi10Mg parts fabricated by selective laser melting. J Mater Process Technol 241:154–163

110. Ferrar B et al (2012) Gas flow effects on selective laser melting (SLM) manufacturing performance. J Mater Process Technol 212(2):355–364

111. Dai D, Gu D (2015) Effect of metal vaporization behavior on keyhole-mode surface morphology of selective laser melted composites using different protective atmospheres. Appl Surf Sci 355:310–319

112. Calta NP et al (2020) Pressure dependence of the laser-metal interaction under laser powder bed fusion conditions probed by in situ X-ray imaging. Addit Manuf 32:101084

113. Tan P, Kiran R, Zhou K (2021) Effects of sub-atmospheric pressure on keyhole dynamics and porosity in products fabricated by selective laser melting. J Manuf Process 64:816–827

114. Cooke S et al (2020) Metal additive manufacturing: technology, metallurgy and modelling. J Manuf Process 57:978–1003

115. Le Dantec M et al (2020) Impact of oxygen content in powders on the morphology of the laser molten tracks in preparation for additive manufacturing of silicon. Powder Technol 361:704–710

116. Mertens R et al (2018) Application of base plate preheating during selective laser melting. Procedia CIRP 74:5–11

117. Borisov E et al (2020) Selective laser melting of Inconel 718 under high laser power. Mater Today: Proc

118. Geenen K et al (2019) Microstructure, mechanical, and tribological properties of M3: 2 high-speed steel processed by selective laser melting, hot-isostatic pressing, and casting. Addit Manuf 28:585–599

119. Krell J et al (2018) General investigations on processing tool steel X40CrMoV5-1 with selective laser melting. J Mater Process Technol 255:679–688

120. Tillmann W et al (2020) Tribo-mechanical properties and adhesion behavior of DLC coatings sputtered onto 36NiCrMo16 produced by selective laser melting. Surf Coat Technol 125748

121. Sochalski-Kolbus L et al (2015) Comparison of residual stresses in Inconel 718 simple parts made by electron beam melting and direct laser metal sintering. Metall Mater Trans A 46(3):1419–1432

122. Doubenskaia M et al (2018) Study of selective laser melting of intermetallic TiAl powder using integral analysis. Int J Mach Tools Manuf 129:1–14

123. Rombouts M et al (2004) Production and properties of dense iron based parts produced by laser melting with plasma formation. Proc Powder Metall World Congr

124. Liu Q et al (2015) Effect of high-temperature preheating on the selective laser melting of yttria-stabilized zirconia ceramic. J Mater Process Technol 222:61–74

125. Domashenkov A et al (2017) Selective laser melting of NiTi powder, in Lasers in Manuf Conf 2017

126. Li X et al (2016) Selective laser melting of aluminium metal matrix composites. Proc 2nd Intl Conf Prog Addit Manuf. Research Publishing: Singapore 33–438

127. Papadakis L, Chantzis D, Salonitis K (2018) On the energy efficiency of pre-heating methods in SLM/SLS processes. Int J Adv Manuf Technol 95(1–4):1325–1338

128. Malý M et al (2019) Effect of process parameters and high-temperature preheating on residual stress and relative density of Ti6Al4V processed by selective laser melting. Materials 12(6):930

129. Mertens R et al (2016) Influence of powder bed preheating on microstructure and mechanical properties of H13 tool steel SLM parts. Phys Procedia 83:882–890

130. Yasa E, Kruth J-P, Deckers J (2011) Manufacturing by combining selective laser melting and selective laser erosion/laser re-melting. CIRP Ann 60(1):263–266

131. Griffiths S et al (2018) Effect of laser rescanning on the grain microstructure of a selective laser melted Al-Mg-Zr alloy. Mater Charact 143:34–42

132. Aboulkhair NT et al (2019) 3D printing of aluminium alloys: additive manufacturing of aluminium alloys using selective laser melting. Prog Mater Sci 106:100578

133. Xiao Z et al (2020) Effect of rescanning cycles on the characteristics of selective laser melting of Ti6Al4V. Opt Laser Technol 122:105890

134. Li X et al (2014) The role of a low-energy–density re-scan in fabricating crack-free Al85Ni5Y6Co2Fe2 bulk metallic glass composites via selective laser melting. Mater Des 63:407–411

135. Miao X et al (2020) Effect of laser rescanning on the characteristics and residual stress of selective laser melted titanium Ti6Al4V alloy. Materials 13(18):3940

136. Maleki E et al (2020) Surface post-treatments for metal additive manufacturing: progress, challenges, and opportunities. Addit Manuf 101619

137. Lizzul L et al (2020) Anisotropy effect of additively manufactured Ti6Al4V titanium alloy on surface quality after milling. Precis Eng 67:301–310

138. Alghamdi F et al (2020) Post heat treatment of additive manufactured AlSi10Mg: on silicon morphology, texture and small-scale properties. Mater Sci Eng: A 139296

139. Nicoletto G et al (2017) Influence of post fabrication heat treatments on the fatigue behavior of Ti-6Al-4V produced by selective laser melting. Procedia Struct Integr 7:133–140

140. Cheruvathur S, Lass EA, Campbell CE (2016) Additive manufacturing of 17–4 PH stainless steel: post-processing heat treatment to achieve uniform reproducible microstructure. Jom 68(3):930–942

141. Xu W et al (2015) Additive manufacturing of strong and ductile Ti–6Al–4V by selective laser melting via in situ martensite decomposition. Acta Mater 85:74–84

142. Salmi A et al (2017) Experimental analysis of residual stresses on AlSi10Mg parts produced by means of selective laser melting (SLM). Procedia CIRP 62:458–463

143. Benedetti M et al (2017) The effect of post-sintering treatments on the fatigue and biological behavior of Ti-6Al-4V ELI parts made by selective laser melting. J Mech Behav Biomed Mater 71:295–306

144. Soro N et al (2020) Surface and morphological modification of selectively laser melted titanium lattices using a chemical post treatment. Surf Coat Technol 125794

145. Zhang Y, Li J, Che S (2018) Electropolishing mechanism of Ti-6Al-4V alloy fabricated by selective laser melting. Int J Electrochem Sci 13(5):4792–4807

146. van Hengel IA et al (2017) Data on the surface morphology of additively manufactured Ti-6Al-4V implants during processing by plasma electrolytic oxidation. Data Brief 13:385–389

147. Yang L et al (2020) Surface integrity induced in machining additively fabricated nickel alloy Inconel 625. Procedia CIRP 87:351–354

148. Ni C et al (2020) Effects of machining surface and laser beam scanning strategy on machinability of selective laser melted Ti6Al4V alloy in milling. Mater Des 108880

149. Khaliq W et al (2020) Tool wear, surface quality, and residual stresses analysis of micro-machined additive manufactured Ti–6Al–4V under dry and MQL conditions. Tribol Int 106408

150. Vaithilingam J et al (2016) Surface chemistry of Ti6Al4V components fabricated using selective laser melting for biomedical applications. Mater Sci Eng: C 67:294–303

151. Siddique S et al (2015) Influence of process-induced microstructure and imperfections on mechanical properties of AlSi12 processed by selective laser melting. J Mater Process Technol 221:205–213

152. Edwards P, Ramulu M (2014) Fatigue performance evaluation of selective laser melted Ti–6Al–4V. Mater Sci Eng: A 598:327–337

153. Brandl E et al (2012) Additive manufactured AlSi10Mg samples using selective laser melting (SLM): microstructure, high cycle fatigue, and fracture behavior. Mater Des 34:159–169

154. Al-Rubaie KS et al (2020) Machinability of SLM-produced Ti6Al4V titanium alloy parts. J Manuf Process 57:768–786

155. Didier P et al (2021) Consideration of SLM additive manufacturing supports on the stability of flexible structures in finish milling. J Manuf Process 62:213–220

156. Nagalingam AP, Yeo S (2020) Surface finishing of additively manufactured Inconel 625 complex internal channels: a case study using a multi-jet hydrodynamic approach. Addit Manuf 36:101428

157. Nagalingam AP, Lee J-Y, Yeo S (2020) Multi-jet hydrodynamic surface finishing and X-ray computed tomography (X-CT) inspection of laser powder bed fused Inconel 625 fuel injection/ spray nozzles. J Mater Process Technol 117018

158. Nagarajan B et al (2019) Development of micro selective laser melting: the state of the art and future perspectives. Engineering 5(4):702–720

159. Wang X et al (2016) Finishing of additively manufactured metal parts by abrasive flow machining. Proc 27th Annu Int Solid Free Fabr Symp Austin TX

160. Guo J et al (2020) Internal surface quality enhancement of selective laser melted Inconel 718 by abrasive flow machining. J Manuf Sci Eng 142(10)

161. El Hassanin A et al (2020) Rotation-assisted abrasive fluidised bed machining of AlSi10Mg parts made through selective laser melting technology. Procedia Manuf 47:1043–1049

162. Balyakin A, Goncharov E (2020) Hydroabrasive machining of internal channels of parts obtained by SLM. IOP Conf Ser: Mater Sci Eng. IOP Publishing

163. Gilmore R (2018) An evaluation of ultrasonic shot peening and abrasive flow machining as surface finishing processes for selective laser melted 316L

164. Han S et al (2020) Effect of abrasive flow machining (AFM) finish of selective laser melting (SLM) internal channels on fatigue performance. J Manuf Process 59:248–257

165. Guo J et al (2018) On the machining of selective laser melting CoCrFeMnNi high-entropy alloy. Mater Des 153:211–220

166. Golubeva A et al (2017) Research of the possibility of using an electrical discharge machining metal powder in selective laser melting. IOP Conf Ser: Mater Sci Eng. IOP Publishing

167. Fette M et al (2015) Optimized and cost-efficient compression molds manufactured by selective laser melting for the production of thermoset fiber reinforced plastic aircraft components. Procedia CIRP 35:25–30

168. Rickenbacher L, Spierings A, Wegener K (2013) An integrated cost-model for selective laser melting (SLM). Rapid Prototyp J

169. Hassanin H et al (2016) Manufacturing of Ti–6Al–4V microimplantable parts using hybrid selective laser melting and micro-electrical discharge machining. Adv Eng Mater 18(9):1544–1549

170. Zhao C, Qu N, Tang X (2021) Removal of adhesive powders from additive-manufactured internal surface via electrochemical machining with flexible cathode. Precis Eng 67:438–452

171. Zhao C, Qu N, Tang X (2021) Electrochemical mechanical polishing of internal holes created by selective laser melting. J Manuf Process 64:1544–1562

172. Buchbinder D et al (2014) Investigation on reducing distortion by preheating during manufacture of aluminum components using selective laser melting. J Laser Appl 26(1):012004

173. Berger U, Merkel M, Liebisch A (2016) The influence of preheating on laser beam melting. Proc 2nd Intl Conf Progress Addit Manuf. Singapore 306–311

174. Siddique S, Imran M, Walther F (2017) Very high cycle fatigue and fatigue crack propagation behavior of selective laser melted AlSi12 alloy. Int J Fatigue 94:246–254

175. Prashanth K, Scudino S, Eckert J (2017) Defining the tensile properties of Al-12Si parts produced by selective laser melting. Acta Mater 126:25–35

176. Olakanmi EO, Cochrane R, Dalgarno K (2015) A review on selective laser sintering/melting (SLS/SLM) of aluminium alloy powders: processing, microstructure, and properties. Prog Mater Sci 74:401–477

177. Molaei R, Fatemi A (2018) Fatigue design with additive manufactured metals: issues to consider and perspective for future research. Procedia engineering 213:5–16

178. Vayssette B et al (2020) Surface roughness effect of SLM and EBM Ti-6Al-4V on multiaxial high cycle fatigue. Theoret Appl Fract Mech 108:102581

179. El Haddad M, Topper T, Smith K (1979) Prediction of non propagating cracks. Eng Fract Mech 11(3):573–584

180. Murakami Y, Endo M (1994) Effects of defects, inclusions and inhomogeneities on fatigue strength. Int J Fatigue 16(3):163–182

181. Taylor D, Bologna P, Knani KB (2000) Prediction of fatigue failure location on a component using a critical distance method. Int J Fatigue 22(9):735–742

182. El May M et al (2015) Non-local high cycle fatigue strength criterion for metallic materials with corrosion defects. Fatigue Fract Eng Mater Struct 38(9):1017–1025

183. Pessard E et al (2013) A mechanistic approach to the Kitagawa-Takahashi diagram using a multiaxial probabilistic framework. Eng Fract Mech 109:89–104

184. Le V-D et al (2016) Simulation of the Kitagawa-Takahashi diagram using a probabilistic approach for cast Al-Si alloys under different multiaxial loads. Int J Fatigue 93:109–121

185. Wilson P et al (2019) Isothermal fatigue damage mechanisms at ambient and elevated temperature of a cast Al-Si-Cu aluminium alloy. Int J Fatigue 121:112–123

186. Vayssette B et al (2019) Numerical modelling of surface roughness effect on the fatigue behavior of Ti-6Al-4V obtained by additive manufacturing. Int J Fatigue 123:180–195

187. Gong H et al (2014) Analysis of defect generation in Ti–6Al–4V parts made using powder bed fusion additive manufacturing processes. Addit Manuf 1:87–98

188. Beretta S, Romano S (2017) A comparison of fatigue strength sensitivity to defects for materials manufactured by AM or traditional processes. Int J Fatigue 94:178–191

189. Meneghetti G, Rigon D, Gennari C (2019) An analysis of defects influence on axial fatigue strength of maraging steel

specimens produced by additive manufacturing. Int J Fatigue 118:54–64

190. Wang Y, Bergström J, Burman C (2006) Four-point bending fatigue behaviour of an iron-based laser sintered material. Int J Fatigue 28(12):1705–1715

191. Vayssette B et al (2018) Surface roughness of Ti-6Al-4V parts obtained by SLM and EBM: effect on the high cycle fatigue life. Procedia Eng 213:89–97

192. Koutiri I et al (2018) Influence of SLM process parameters on the surface finish, porosity rate and fatigue behavior of as-built Inconel 625 parts. J Mater Process Technol 255:536–546

193. Leon A, Aghion E (2017) Effect of surface roughness on corrosion fatigue performance of AlSi10Mg alloy produced by selective laser melting (SLM). Mater Charact 131:188–194

194. Günther J et al (2018) On the effect of internal channels and surface roughness on the high-cycle fatigue performance of Ti-6Al-4V processed by SLM. Mater Des 143:1–11

195. Mower TM, Long MJ (2016) Mechanical behavior of additive manufactured, powder-bed laser-fused materials. Mater Sci Eng: A 651:198–213

196. Meier C et al (2019) Critical influences of particle size and adhesion on the powder layer uniformity in metal additive manufacturing. J Mater Process Technol 266:484–501

197. Adams RD (2005) Adhesive bonding: science, technology and applications. Elsevier

198. Kinloch AJ (2012) Adhesion and adhesives: science and technology. Springer Sci Bus Media

199. Fielden-Stewart Z et al (2021) Effect of the surface morphology of SLM printed aluminium on the interfacial fracture toughness of metal-composite hybrid joints. Int J Adhes Adhes 105:102779

200. Zhang B et al (2012) Improvement of surface properties of SLM parts by atmospheric plasma spraying coating. Appl Surf Sci 263:777–782

201. Riemer A et al (2014) On the fatigue crack growth behavior in 316L stainless steel manufactured by selective laser melting. Eng Fract Mech 120:15–25

202. Fayazfar H et al (2018) A critical review of powder-based additive manufacturing of ferrous alloys: process parameters, microstructure and mechanical properties. Mater Des 144:98–128

203. Hanzl P et al (2015) The influence of processing parameters on the mechanical properties of SLM parts. Procedia Eng 100(1):1405–1413

204. Kempen K et al (2012) Mechanical properties of AlSi10Mg produced by selective laser melting. Phys Procedia 39:439–446

205. Zebarjad SM, Sajjadi S (2006) Microstructure evaluation of Al–Al2O3 composite produced by mechanical alloying method. Mater Des 27(8):684–688

206. Dolata-Grosz A, Śleziona J, Formanek B (2006) Structure and properties of aluminium cast composites strengthened by dispersion phases. J Mater Process Technol 175(1–3):192–197

207. Wang Z et al (2020) Modified wear behavior of selective laser melted Ti6Al4V alloy by direct current assisted ultrasonic surface rolling process. Surf Coat Technol 381:125122

208. Amanov A, Pyun Y-S (2017) Local heat treatment with and without ultrasonic nanocrystal surface modification of Ti-6Al-4V alloy: mechanical and tribological properties. Surf Coat Technol 326:343–354

209. Delgado J, Ciurana J, Rodríguez CA (2012) Influence of process parameters on part quality and mechanical properties for DMLS and SLM with iron-based materials. Int J Adv Manuf Technol 60(5–8):601–610

210. Hitzler L et al (2017) On the anisotropic mechanical properties of selective laser-melted stainless steel. Materials 10(10):1136

211. Vilaro T, Colin C, Bartout J-D (2011) As-fabricated and heat-treated microstructures of the Ti-6Al-4V alloy processed by selective laser melting. Metall Mater Trans A 42(10):3190–3199

212. Vrancken B et al (2012) Heat treatment of Ti6Al4V produced by selective laser melting: microstructure and mechanical properties. J Alloy Compd 541:177–185

213. Sustarsic B et al (2009) Microstructure and mechanical characteristics of DMLS tool-inserts. Mater Manuf Process 24(7–8):837–841

214. Wang Y, Bergström J, Burman C (2009) Thermal fatigue behavior of an iron-based laser sintered material. Mater Sci Eng: A 513:64–71

215. Attar H et al (2014) Manufacture by selective laser melting and mechanical behavior of commercially pure titanium. Mater Sci Eng: A 593:170–177

216. Zhang L et al (2011) Manufacture by selective laser melting and mechanical behavior of a biomedical Ti–24Nb–4Zr–8Sn alloy. Scripta Mater 65(1):21–24

217. Wang Z et al (2012) The microstructure and mechanical properties of deposited-IN718 by selective laser melting. J Alloy Compd 513:518–523

218. Amato K et al (2012) Microstructures and mechanical behavior of Inconel 718 fabricated by selective laser melting. Acta Mater 60(5):2229–2239

219. Yadroitsev I et al (2007) Strategy of manufacturing components with designed internal structure by selective laser melting of metallic powder. Appl Surf Sci 254(4):980–983

220. Pantělejev L et al (2017) Mechanical and microstructural properties of 2618 al-alloy processed by SLM remelting strategy. Mater Sci Forum. Trans Tech Publ

221. Guan K et al (2013) Effects of processing parameters on tensile properties of selective laser melted 304 stainless steel. Mater Des 50:581–586

222. Murr LE et al (2011) Microstructural architecture, microstructures, and mechanical properties for a nickel-base superalloy fabricated by electron beam melting. Metall Mater Trans A 42(11):3491–3508

223. Zhao X et al (2008) Study on microstructure and mechanical properties of laser rapid forming Inconel 718. Mater Sci Eng: A 478(1–2):119–124

224. Yadroitsev I et al (2009) Mechanical properties of samples fabricated by selective laser melting. 14èmes Assises Européennes du Prototypage Fabr Rapide

225. Geetha M et al (2009) Ti based biomaterials, the ultimate choice for orthopaedic implants–a review. Prog Mater Sci 54(3):397–425

226. Bathini U et al (2010) A study of the tensile deformation and fracture behavior of commercially pure titanium and titanium alloy: influence of orientation and microstructure. J Mater Eng Perform 19(8):1172–1182

227. Baufeld B (2012) Mechanical properties of Inconel 718 parts manufactured by shaped metal deposition (SMD). J Mater Eng Perform 21(7):1416–1421

228. Zhang S et al (2009) Fatigue properties of a multifunctional titanium alloy exhibiting nonlinear elastic deformation behavior. Scripta Mater 60(8):733–736

229. Li Y et al (2014) New developments of Ti-based alloys for biomedical applications. Materials 7(3):1709–1800

230. Kurgan N (2013) Effects of sintering atmosphere on microstructure and mechanical property of sintered powder metallurgy 316L stainless steel. Mater Des (1980-2015) 52:995–998

231. Saboori A et al (2018) Effect of graphene nanoplatelets on microstructure and mechanical properties of AlSi10Mg nanocomposites produced by hot extrusion. Powder Metall Met Ceram 56(11–12):647–655

232. Lumley R (2008) Technical data sheets for heat-treated aluminum high-pressure die castings. Die Cast Eng 32

233. Bajoraitis R (1988) Forming of titanium and titanium alloys. ASM Handbook 14:838–848

234. Majeed A et al (2020) Investigation of T4 and T6 heat treatment influences on relative density and porosity of AlSi10Mg alloy components manufactured by SLM. Comput Ind Eng 139:106194

235. Uzun M, Usca UA (2018) Effect of Cr particulate reinforcements in different ratios on wear performance and mechanical properties of Cu matrix composites. J Braz Soc Mech Sci Eng 40(4):197

236. Zhang B et al (2016) Microhardness and microstructure evolution of TiB2 reinforced Inconel 625/TiB2 composite produced by selective laser melting. Opt Laser Technol 80:186–195

237. Kluczyński J et al (2018) The influence of exposure energy density on porosity and microhardness of the SLM additive manufactured elements. Materials 11(11):2304

238. Buchbinder D et al (2011) High power selective laser melting (HP SLM) of aluminum parts. Phys Procedia 12:271–278

239. Yusuf SM et al (2017) Investigation on porosity and microhardness of 316L stainless steel fabricated by selective laser melting. Metals 7(2):64

240. Li XP et al (2017) Selective laser melting of nano-TiB2 decorated AlSi10Mg alloy with high fracture strength and ductility. Acta Mater 129:183–193

241. Dadbakhsh S, Hao L (2012) Effect of Al alloys on selective laser melting behaviour and microstructure of in situ formed particle reinforced composites. J Alloy Compd 541:328–334

242. AlMangour B, Grzesiak D, Yang J-M (2016) Rapid fabrication of bulk-form TiB2/316L stainless steel nanocomposites with novel reinforcement architecture and improved performance by selective laser melting. J Alloy Compd 680:480–493

243. Gu D et al (2012) Selective laser melting of TiC/Ti bulk nanocomposites: influence of nanoscale reinforcement. Scripta Mater 67(2):185–188

244. Wang L et al (2020) Adhesion effects on spreading of metal powders in selective laser melting. Powder Technol 363:602–610

245. Eyzat Y et al (2019) Characterization and mechanical properties of as-built SLM Ti-6Al-4V subjected to surface mechanical post-treatment. Procedia CIRP 81:1225–1229

246. Zhao X et al (2020) Combined effect of TiN coating and surface texture on corrosion-wear behavior of selective laser melted CP-titanium in simulated body fluid. J Alloy Compd 816:152667

247. Cutolo A et al (2023) Fatigue life prediction of a L-PBF component in Ti-6Al-4V using sample data, FE-based simulations and machine learning. Int J Fatigue 167:107276

248. Mandal V et al (2023) Fabrication of ex-situ TiN reinforced IN718 composites using laser powder bed fusion (L-PBF): experimental characterization and high-fidelity numerical simulations. Ceram Int

249. Jiabao H et al (2023) Surface morphology evolution of GTD-450 stainless steel during laser powder bed fusion. Vacuum 112107

250. Li C et al (2023) Surface characteristics enhancement and morphology evolution of selective-laser-melting (SLM) fabricated stainless steel 316L by laser polishing. Opt Laser Technol 162:109246

251. Wang Z et al (2023) Anisotropic tension-compression asymmetry in SLM 316L stainless steel. Int J Mech Sci 108139

252. Pilgar CM, Fernandez AM, Segurado J (2023) Microstructure sensitive fatigue life prediction model for SLM fabricated Hastelloy-X. Int J Fatigue 168:107372

253. Long T, Huang H (2023) An improved high order smoothed particle hydrodynamics method for numerical simulations of selective laser melting process. Eng Anal Boundary Elem 147:320–335

254. Peng J et al (2023) Data-driven investigation of microstructure and surface integrity in additively manufactured multi-principal-element alloys. J Alloy Compd 937:168431

Publisher's note Springer Nature remains neutral with regard to jurisdictional claims in published maps and institutional affiliations.

Authors and Affiliations

Mustafa Kuntoğlu[1] · Emin Salur[2] · Eyüb Canli[1] · Abdullah Aslan[1] · Munish Kumar Gupta[3,4] · Saad Waqar[5] · Grzegorz M. Krolczyk[3] · Jinyang Xu[6]

✉ Munish Kumar Gupta
  xujinyang@sjtu.edu.cn

✉ Jinyang Xu
  xujinyang@sjtu.edu.cn

  Mustafa Kuntoğlu
  mkuntoglu@selcuk.edu.tr

  Emin Salur
  esalur@selcuk.edu.tr

  Eyüb Canli
  ecanli@selcuk.edu.tr

  Abdullah Aslan
  aaslan@selcuk.edu.tr

  Saad Waqar
  saad.waqar@polyu.edu.hk

  Grzegorz M. Krolczyk
  G.Krolczyk@po.edu.pl

1 Mechanical Engineering Department, Technology Faculty, Selcuk University, Konya 42130, Turkey

2 Metallurgical and Materials Engineering, Technology Faculty, Selcuk University, Konya 42130, Turkey

3 Faculty of Mechanical Engineering, Opole University of Technology, 76 Proszkowska St, 45-758 Opole, Poland

4 Department of Mechanical Engineering, Graphic Era Deemed to Be University, Uttrakhand, Dehradun, India

5 Department of Industrial and Systems Engineering, Hong Kong Polytechnic University, Kowloon, Hong Kong SAR

6 State Key Laboratory of Mechanical System and Vibration, School of Mechanical Engineering, Shanghai Jiao Tong University, Shanghai 200240, People's Republic of China